Electronic Supplementary Material (ESI) for Organic Chemistry Frontiers.

Supramolecular Vesicle Engineering by Regulating the Assembly of Shape-Persistent Aromatic-Hydrazone Macrocycles

He Deng,[a] Guanfei Gong,[a] Siheng Lv,[a] Yi Chen,[a] Qi Zhao,[a] Shanshan Liu,[a] Shigui Chen,*[a] and Lu Wang*[a]

[a] The Institute for Advanced Studies, and Department of Gastroenterology, Hubei Clinical Center & Key Lab of Intestinal & Colorectal Diseases, Zhongnan Hospital, Wuhan University, Wuhan, Hubei 430072, China

Email: sgchen@whu.edu.cn (Shigui Chen), wanglu-027@whu.edu.cn (Lu Wang).

Electronic Supplementary Information (ESI)

Table of Contents

Materials and Methods

All solvents were dried before use following the standard procedures. Unless indicated otherwise, all starting materials were obtained from commercial suppliers and used without additional purification. Analytical thin-layer chromatography (TLC) was performed on silica-gel plates w/UV254. ^{1}H NMR and ^{13}C NMR spectra were recorded on Bruker AVANCE NEO 600MHz, at a constant temperature of 298.0 K. Chemical shifts are reported in δ values in ppm using residual solvent as internal standard and coupling constants (J) are denoted in Hz. MALDI-TOF MS spectra were recorded on a Bruker autoflex maX spectrometer, matrix is trans-2-[3-(4-tert-Butylphenyl)-2-methyl-2-propenylidene]malononitrile(DCTB). High resolution mass spectra were recorded using ESI ionization in the positive mode on ThermoFisher LTQ-Orbitrap Elite. The morpholgy of supramolecular assemblies was revealed by a high-resolution transmission electron microscope (JEOL JEM-F200) operating at an accelerating voltage of 200 kV. The sample was prepared by dropping the solution onto a carbon-coated copper grid and then was air-dried. The ground state geometries were derived by density functional theory (DFT). All the computations were performed using the Gaussian 09 program on a personal computer using B3LYP and ωB97XD in conjunction with 6-31G (d, p). All analyses as well as drawing of various kinds of maps were finished using the Multiwfn 3.7 code.[S1, S2]

Synthesis of macrocycle MC

Macrocycle **MC**[S3] was synthesized according to the reported literature.

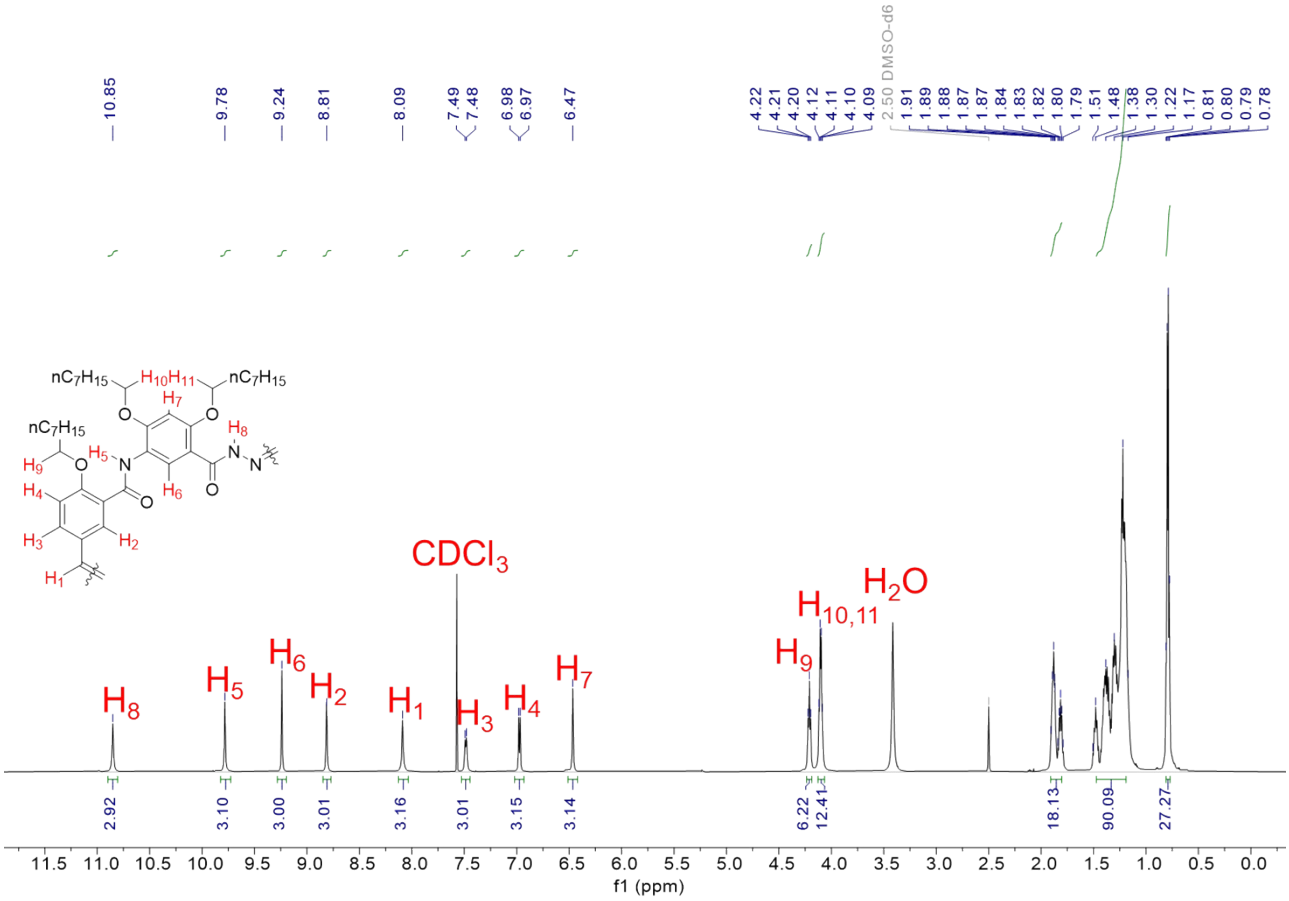

Figure S1. ^{1}H NMR spectrum (600 MHz, $CDCl_3$/DMSO-d_6 = 4/1, v/v, 298.0 K) of **MC**.

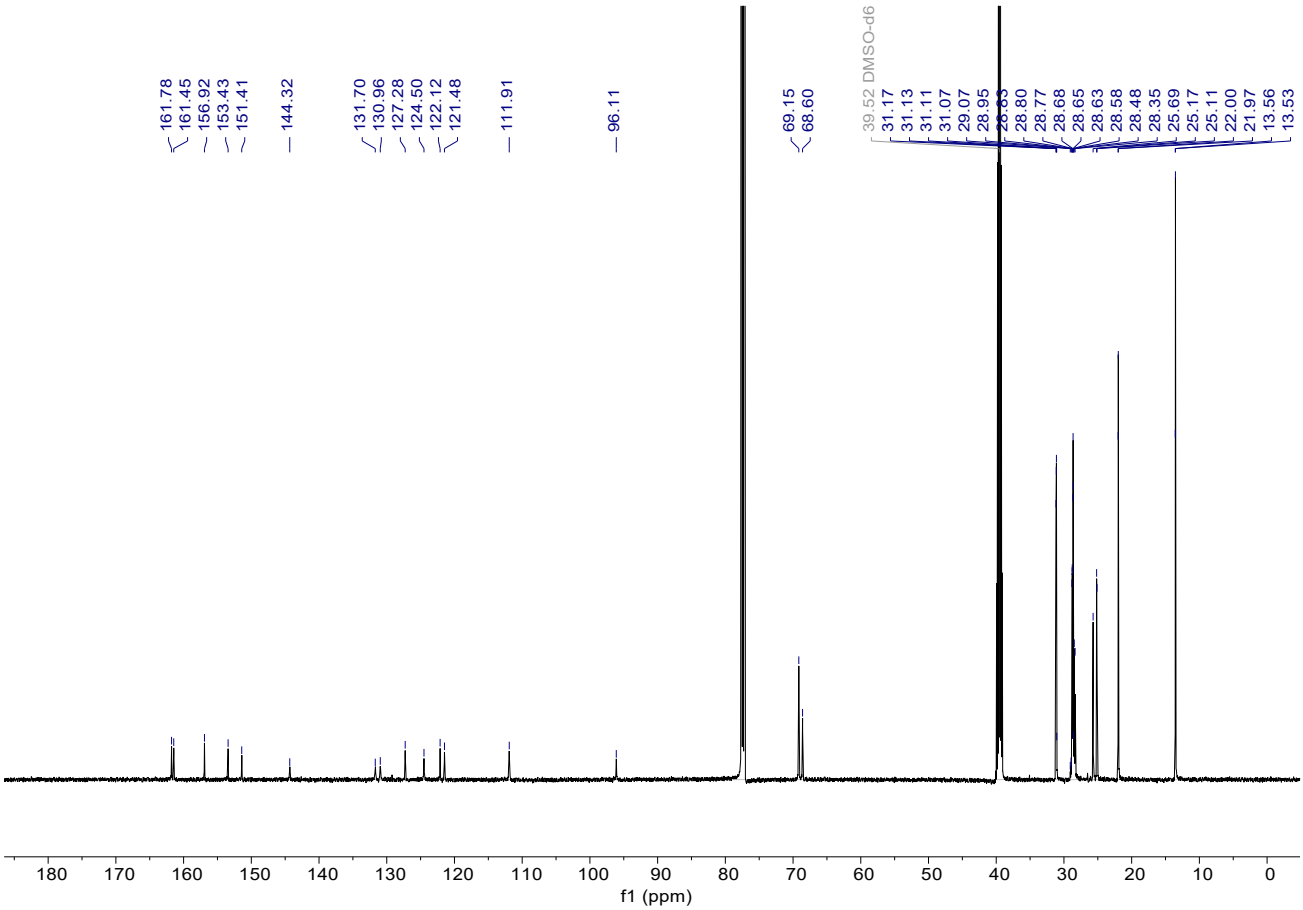

Figure S2. ^{13}C NMR spectrum (600 MHz, $CDCl_3$/DMSO-d_6 = 4/1, v/v, 298.0 K) of **MC**.

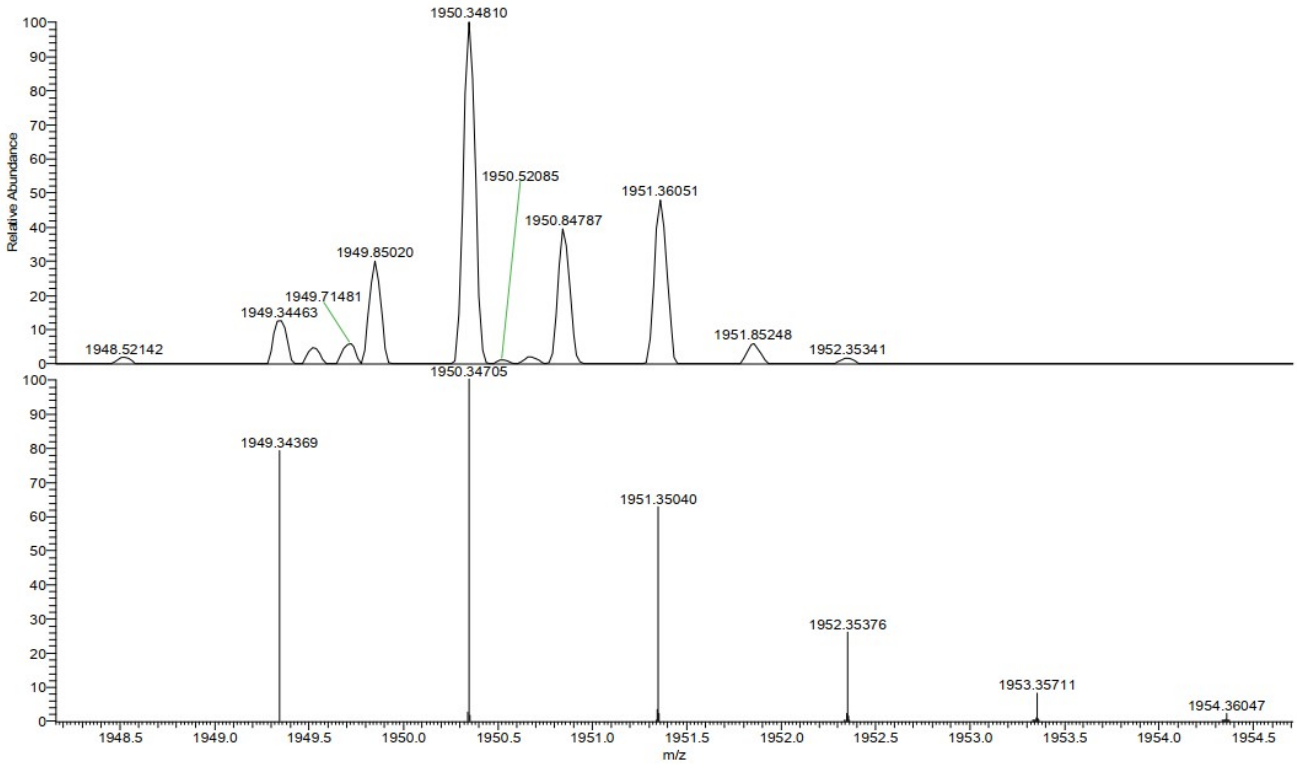

Figure S3. HRMS (ESI)-mass spectrum of **MC** (top: experimental, bottom: simulated).

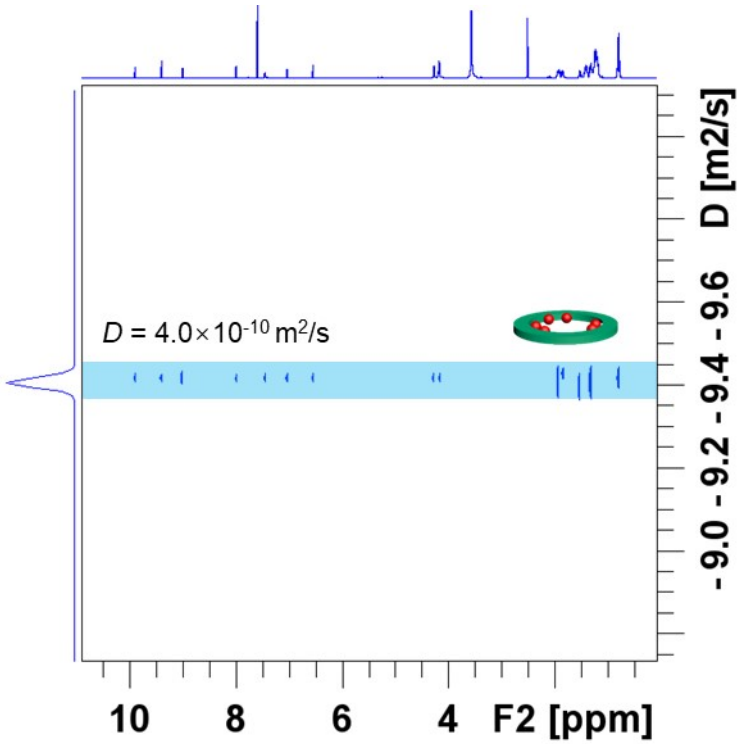

Figure S4. Partial DOSY spectrum (600 MHz, $CDCl_3$/DMSO-d_6 = 4/1, v/v, 298.0 K) of **MC**. [**MC**] = 1.0 mM.

Synthesis of guests MP1, MP2, BP1 and BP2

The synthetic routes of guests are shown in **Scheme S1.**

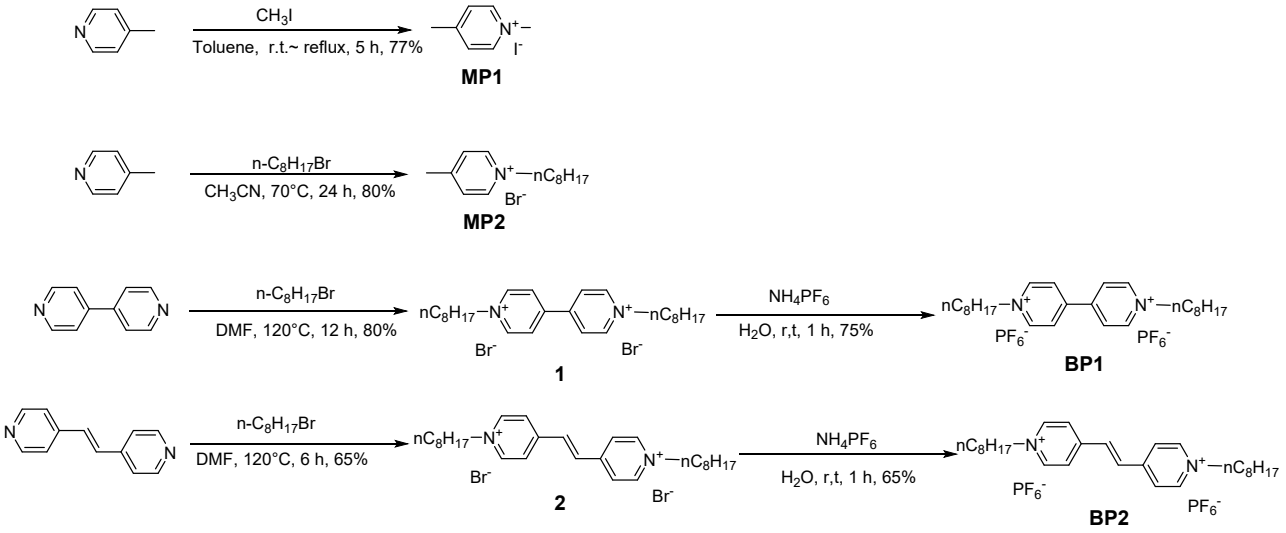

Scheme S1. Synthetic route to Guests

Synthesis of **MP1**[S4]: 4-picoline (93.1 mg, 1.0 mmol, 1.0 eq) and methyl iodide (238.9 mg, 2.0 mmol, 2.0 eq) were mixed in toluene (2 ml). The solution was stirred at room temperature for 4 h, and refluxing for 1h. After cooling, the precipitated **MP1** was filtered and washed with ethyl ether, and was further dried in vacuum for 2 h, the product was collected as light yellow solid (180.1 mg), yield 77.0%. ^{1}H NMR (600 MHz, DMSO-d_6, 298.0 K) δ (ppm): 8.82 (d, J = 6.6 Hz, 2H), 7.95 (d, J = 6.3 Hz, 2H), 4.26 (s, 3H), 2.59 (s, 3H). ^{13}C NMR (150 MHz, DMSO-d_6, 298.0 K) δ (ppm): 158.27, 144.58, 128.01, 47.16, 21.35. HR-ESI MS: calcd for $[M-I]^+$ m/z 108.0808, found m/z 108.0805.

Synthesis of **MP2**[S5]: 4-picoline (93.1 mg, 1.0 mmol, 1.0 eq) and 1-Bromooctane (289.7 mg, 1.5 mmol, 1.5 eq) were mixed in CH_3CN (1 ml). The solution was stirred at 70°C for 24 h. After cooling, solvent was

removed under reduced pressure. The product was purified by column chromatography (SiO_2, $CHCl_2$/MeOH) to obtain compound **MP2** as a yellow viscous solid (228.0 mg), yield 80.0%. ^{1}H NMR (600 MHz, DMSO-d_6, 298.0 K) δ (ppm): 8.93 (d, J = 6.8 Hz, 2H), 7.99 (d, J = 6.2 Hz, 2H), 4.51 (t, J = 7.4 Hz, 2H), 2.60 (s, 3H), 1.87 (m, J = 7.5 Hz, 2H), 1.24 (m, J = 8.1 Hz, 10H), 0.89 – 0.81 (m, 3H). ^{13}C NMR (150 MHz, DMSO-d_6, 298.0 K) δ (ppm): 158.77, 143.76, 128.37, 59.87, 13.99. HR-ESI MS: calcd for $[M-Br]^+$ m/z 206.1903, found m/z 206.1902.

Synthesis of **BP1**[S6]**:** 4,4'-Bipyridine (156.2 mg, 1.0 mmol, 1.0 eq) and 1-Bromooctane (424.9 mg, 2.2 mmol, 2.2 eq) were mixed in N,N-Dimethylformamide (4.0 ml). The solution was stirred at 120°C for 24 h. After cooling, the precipitated **1** was filtered and washed with N,N-Dimethylformamide and ethyl ether, and was further dried in vacuum for 2 h, the product was collected as yellow solid (434.0 mg), yield 80.0%. For anion exchange, an aqueous solution of **1** (434.0 mg, 0.80 mmol, 1.0 mM) was added to the NH_4PF_6 (317.9 mg, 2.0 mmol, 3.0 eq) at room temperature. The mixture was stirred for 1 h, the precipitated **BP1** was filtered and washed with water, and was further dried in vacuum for 24 h, the product was collected as light yellow solid (403.5 mg), yield 75.0%. ^{1}H NMR (600 MHz, DMSO-d_6, 298.0 K) δ (ppm): 9.36 (d, J = 7.0 Hz, 4H), 8.76 (d, J = 7.0 Hz, 4H), 4.67 (t, J = 7.5 Hz, 4H), 1.97 (m, J = 7.2 Hz, 4H), 1.33 – 1.22 (m, 20H), 0.89 – 0.83 (m, 6H). ^{13}C NMR (150 MHz, DMSO-d_6, 298.0 K) δ (ppm): 148.67, 145.76, 126.63, 60.99, 31.16, 30.76, 28.49, 28.39, 25.46, 22.07, 13.97. HR-ESI MS: calcd for $[M-2PF_6]^+$ m/z 191.1669, found m/z 191.1667.

Synthesis of **BP2**[S7]**:** trans-1,2-Di(4-pyridyl)ethylene (182.1 mg, 1.0 mmol, 1.0 eq) and 1-Bromooctane (424.9 mg, 2.2 mmol, 2.2 eq) were mixed in N,N-Dimethylformamide (4 ml). The solution was stirred at 120°C for 24 h. After cooling, the precipitated **2** was filtered and washed with N,N-Dimethylformamide and ethyl ether, and was further dried in vacuum for 2 h, the product was collected as yellow solid (367.9 mg), yield 65.0%. For anion exchange, an aqueous solution of **2** (367.9 mg, 0.65 mmol, 1.0 mM) was added to the NH_4PF_6 (317.9 mg, 2.0 mmol, 3.0 eq) at room temperature. The mixture was stirred for 1 h, the precipitated **BP2** was filtered and washed with water, and was further dried in vacuum for 24 h, the product was collected as light yellow solid (218.0 mg), yield 49.1%. ^{1}H NMR (600 MHz, DMSO-d_6, 298.0 K) δ (ppm): 9.12 (d, J = 6.1 Hz, 4H), 8.33 (d, J = 5.4 Hz, 4H), 8.11 (s, 2H), 4.57 (s, 4H), 1.93 (m, J = 7.3 Hz, 4H), 1.34 – 1.20 (m, 20H), 0.88 – 0.83 (m, 6H). ^{13}C NMR (150 MHz, DMSO-d_6, 298.0 K) δ (ppm): 150.37, 145.19, 134.05, 125.48, 60.48, 31.19, 30.65, 28.51, 28.42, 25.48, 22.11, 14.01. HR-ESI MS: calcd for $[M-PF_6]^+$ m/z 553.3141, found m/z 553.3156.

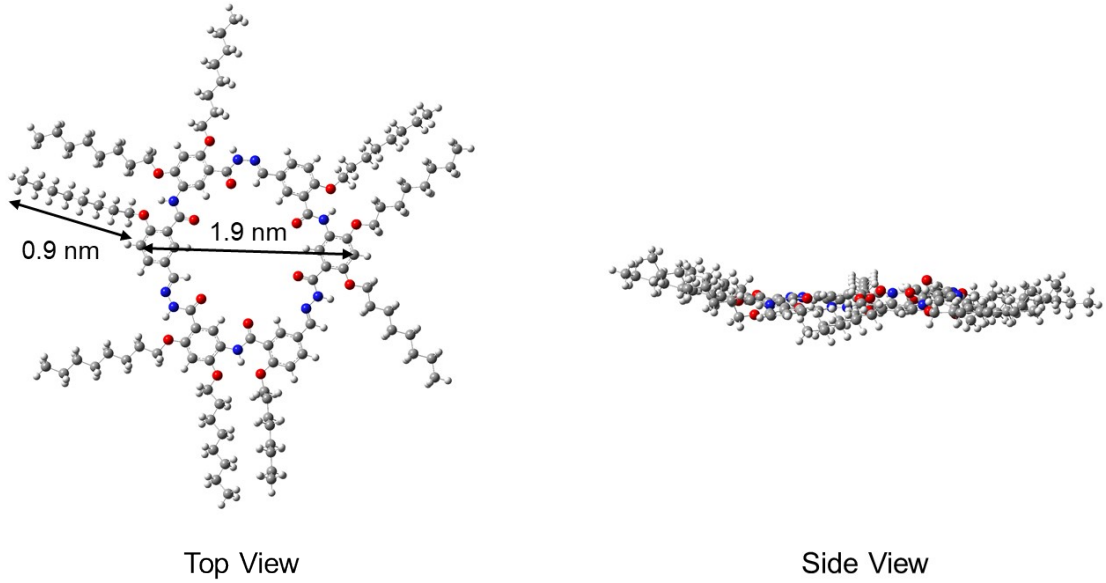

Figure S5. The energy-optimized structure for **MC.**

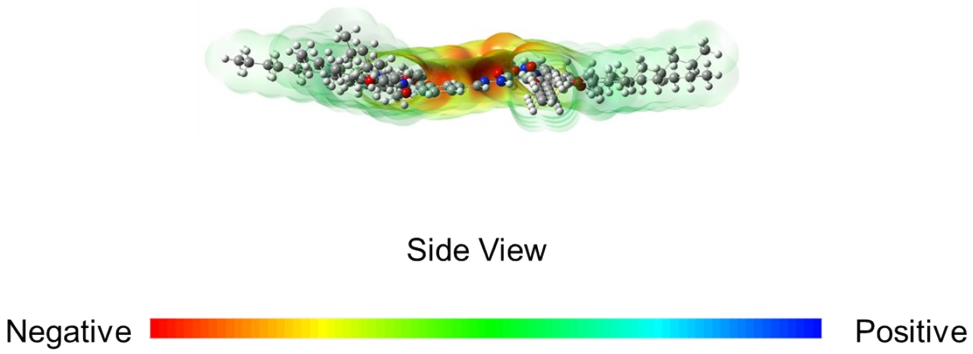

Figure S6. The molecular electrostatic surface potential (ESP) surfaces of Macrocycle **MC**.

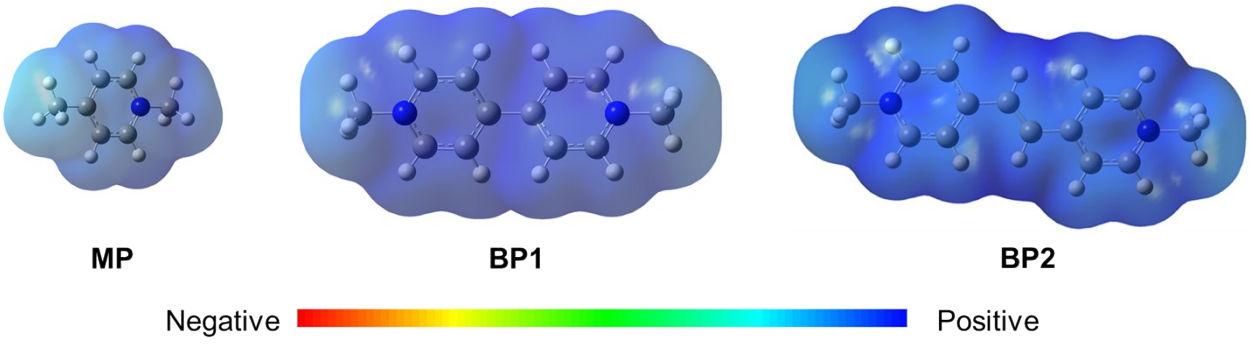

Figure S7. The molecular electrostatic surface potential (ESP) surfaces of guests. (The flexible alkyl chains were omitted for clarity.)

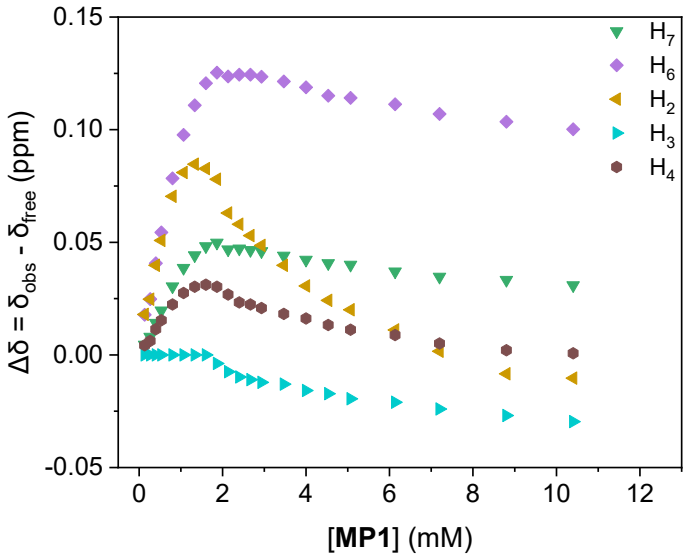

Figure S8. The observed ^{1}H NMR chemical shifts ($\Delta\delta = \delta_{observed} - \delta_{free}$, ppm) of protons in MC.

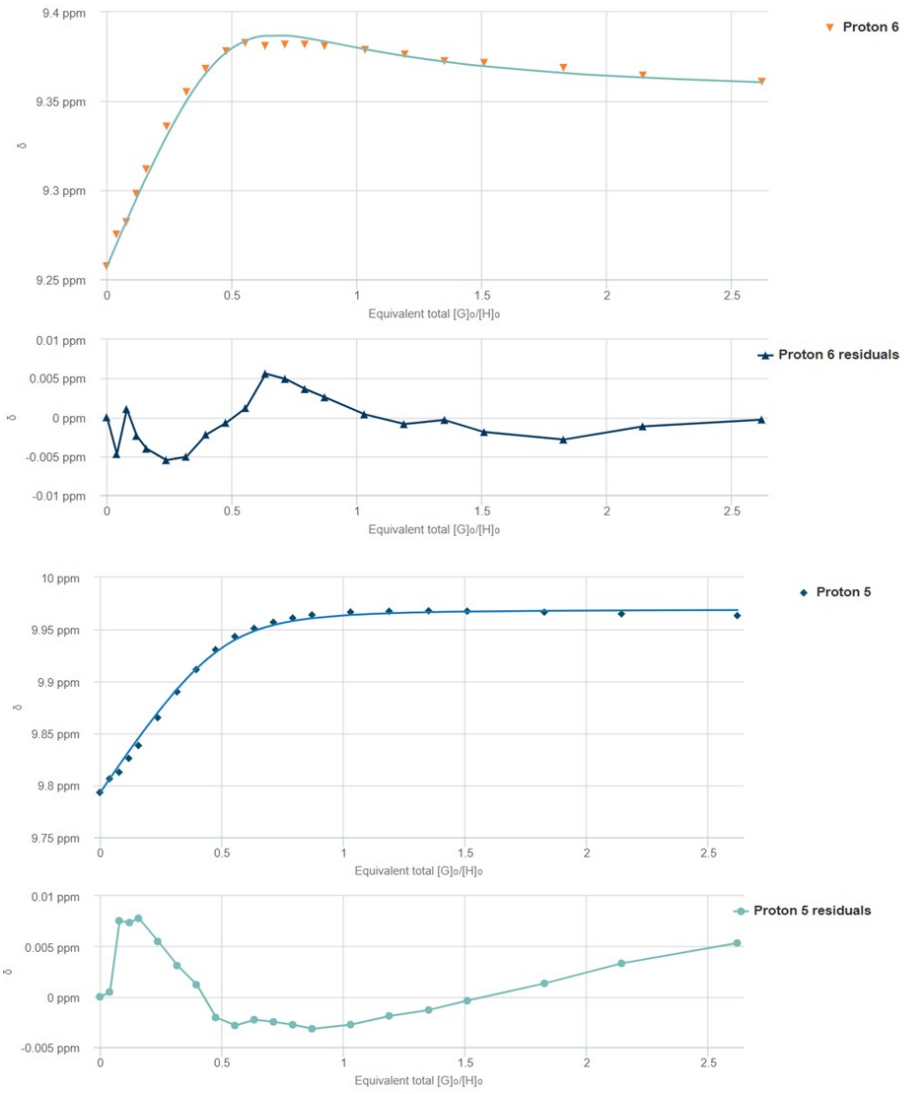

Details

Time to fit	1.7984 s
SSR	2.3816e-3
Fitted datapoints	126
Fitted params	14

Parameters

Parameter (bounds)	Optimised	Error	Initial
K_{11} (0 → ∞)	11669.98 M^{-1}	± 15.2756 %	1000.00 M^{-1}
K_{21} (0 → ∞)	1555.33 M^{-1}	± 8.1310 %	100.00 M^{-1}

Back Next

Figure S9. Nonlinear least-squares analysis of the ^{1}H NMR binding data (**Figure 2a**) corresponding to the formation of **MC_2⊃MP1** complexes. The data were fitted to a 2:1 (host : guest) binding model to give K_{11} = (1.17 ± 0.18) × 10^4 M^{-1} and K_{21} = (1.56 ± 0.13) × 10^3 M^{-1}. The residual distribution is shown below the binding isotherm. All solid lines were obtained from non-linear curve-fitting with the Nelder–Mead method to a 2:1 binding model using the http://supramolecular.org/ web applet.

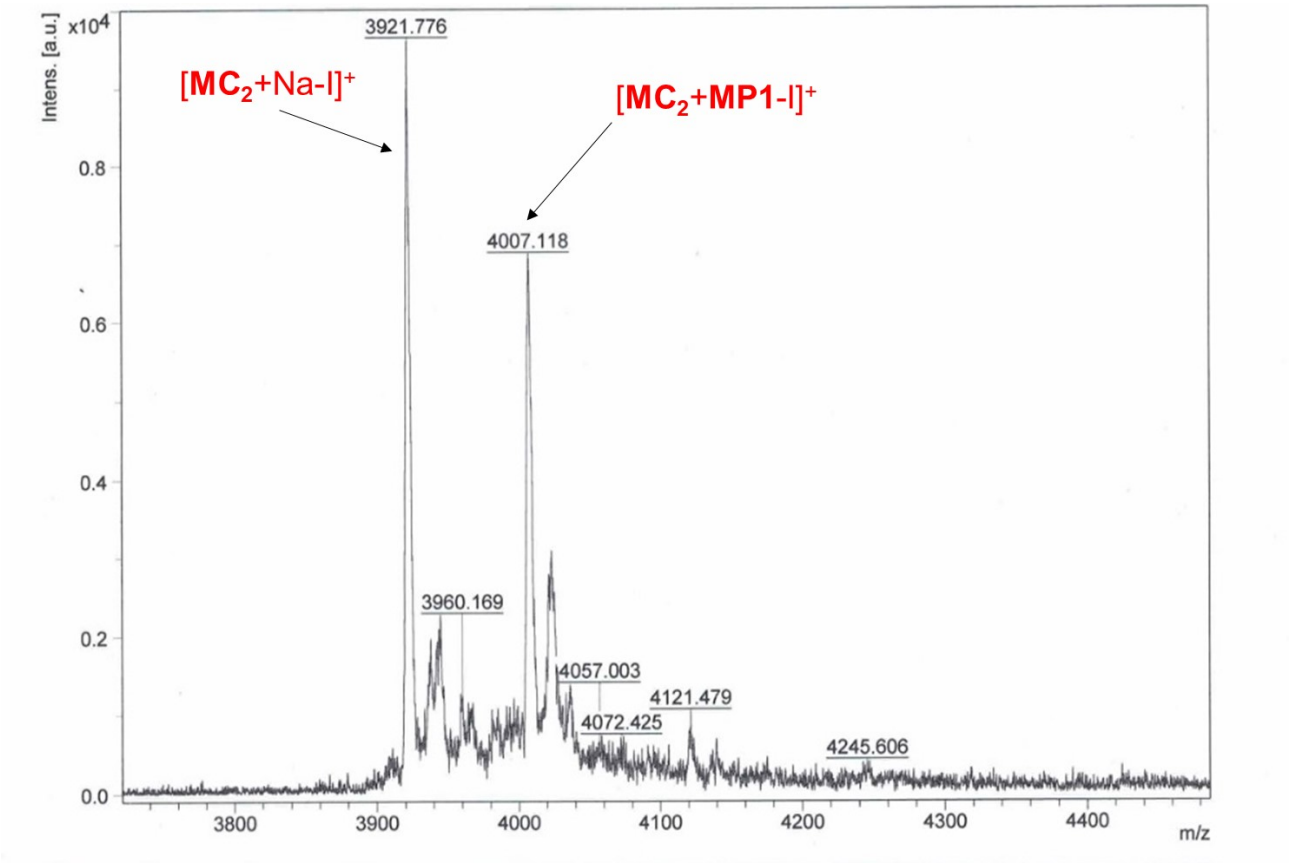

Figure S10. Partial MALDI-TOF-MS spectrum of **MC_2⊃MP1.**

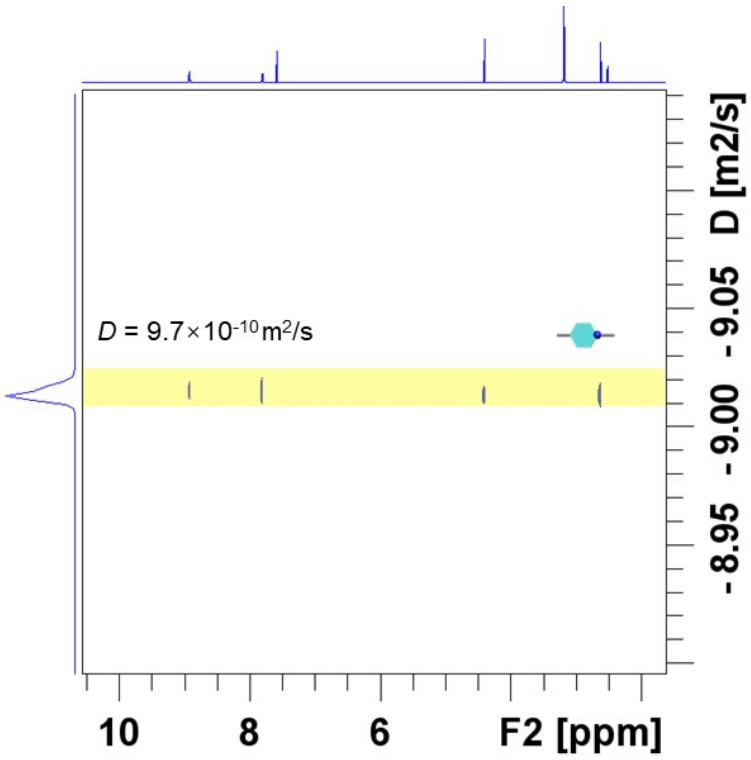

Figure S11. Partial DOSY spectrum (600 MHz, $CDCl_3$/DMSO-d_6 = 4/1, v/v, 298.0 K) of **MP1**. [**MP1**] = 1.0 mM.

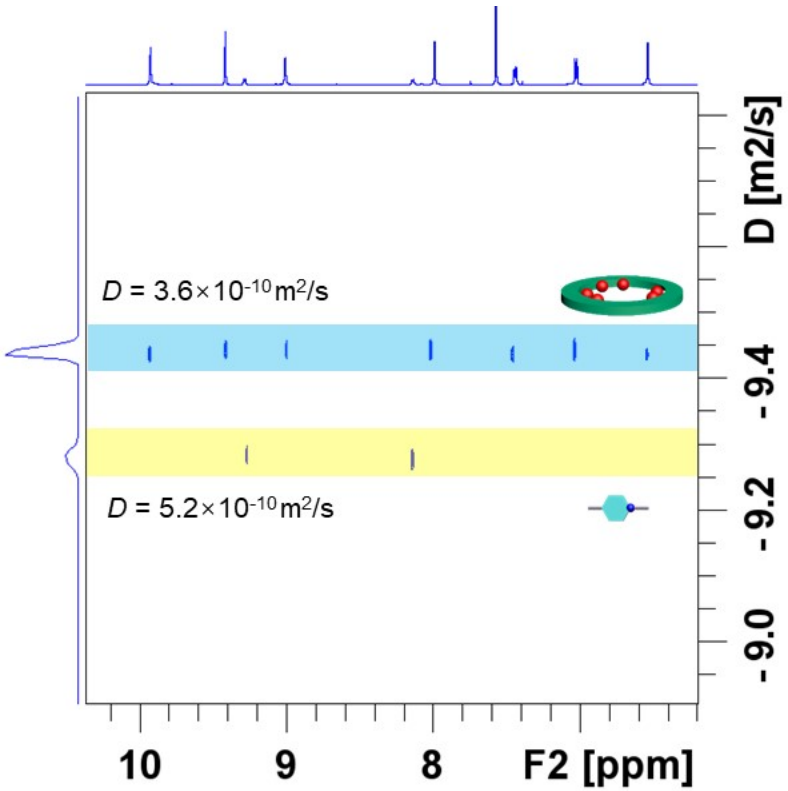

Figure S12. Partial DOSY spectrum (600 MHz, $CDCl_3$/DMSO-d_6 = 4/1, v/v, 298.0 K) of **MC_2⊃MP1**. [**MC**] = 2.0 mM, [**MP1**] = 1.0 mM.

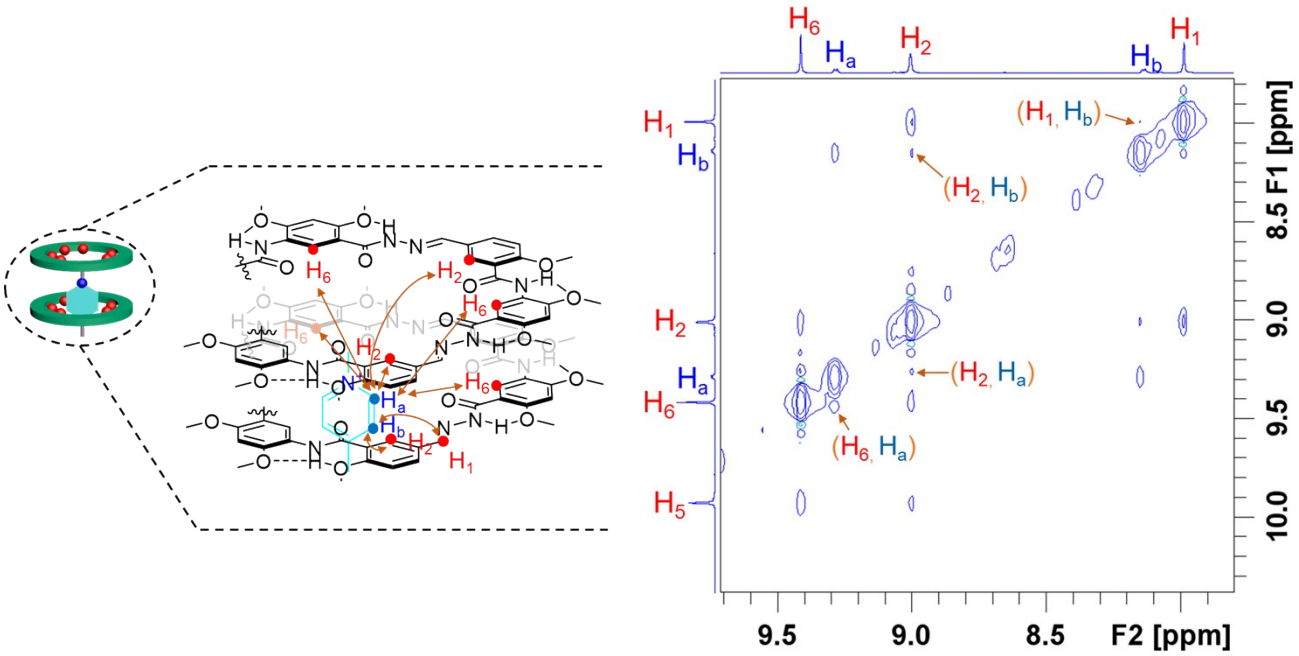

Figure S13. Partial **NOESY spectrum** (600 MHz, $CDCl_3$/DMSO-d_6 = 4/1, v/v, 298.0 K) of **MC_2⊃MP1**. [**MC**] = 2.0 mM, [**MP1**] = 1.0 mM. Arrows represent NOEs between **MC** and **MP1**. (The flexible alkyl chains were omitted for clarity.)

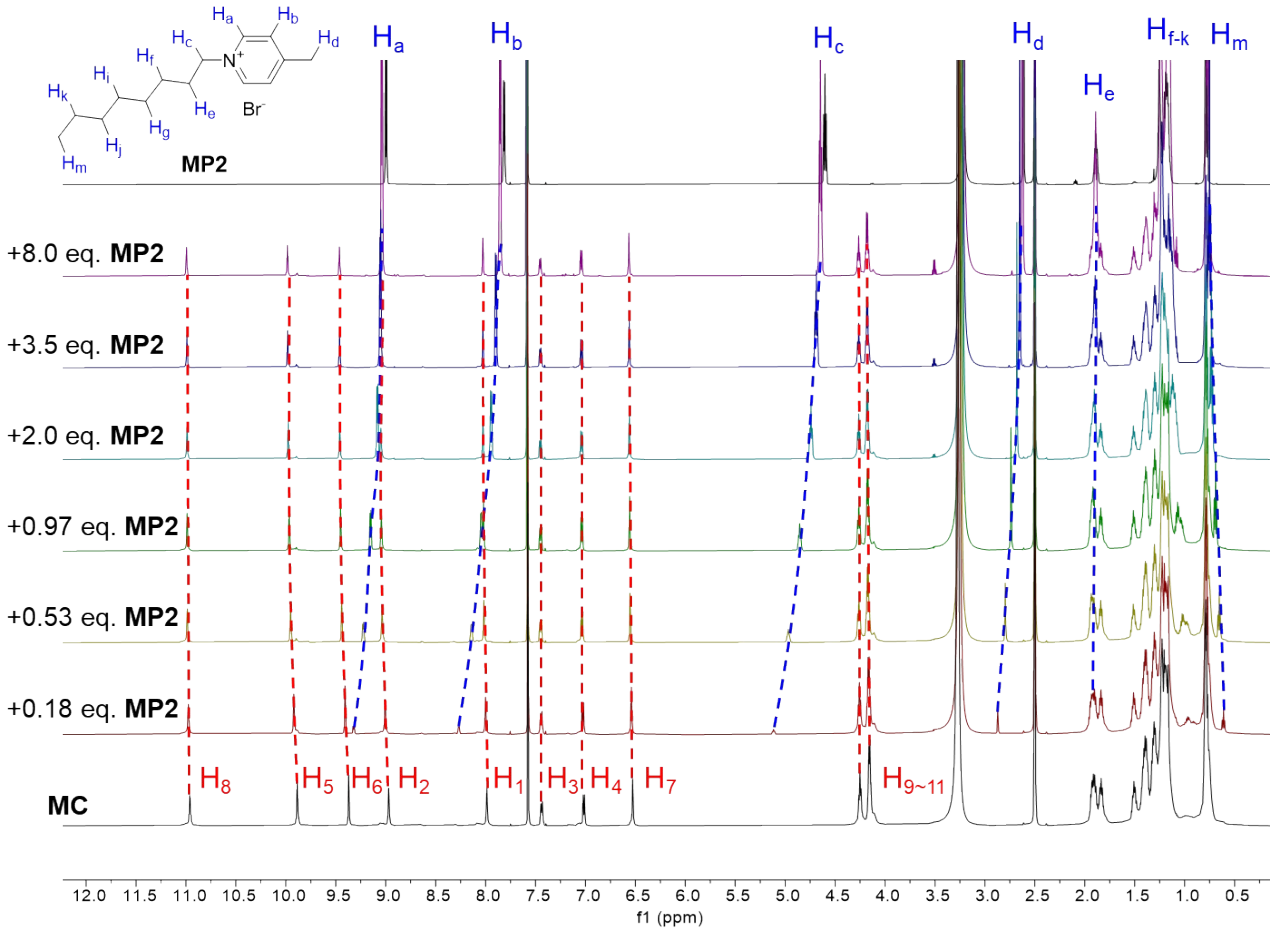

Figure S14. ^{1}H NMR spectra (600 MHz, $CDCl_3$/DMSO-d_6 = 4/1, v/v, 298.0 K) of **MC** at a concentration of 1.0 mM with different equivalent of **MP2**.

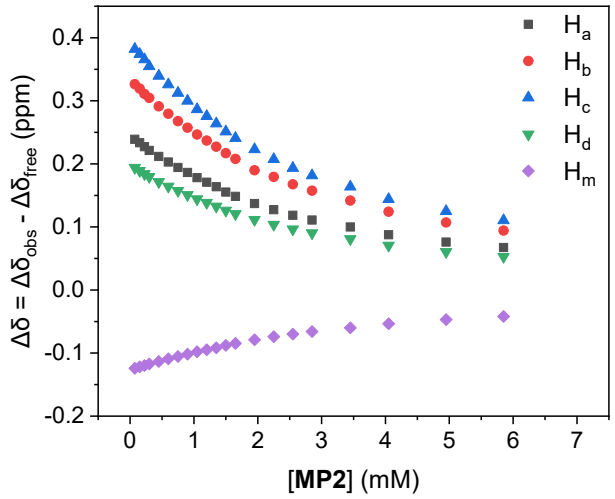

Figure S15. The observed ^{1}H NMR chemical shifts ($\Delta\delta = \delta_{observed} - \delta_{free}$, ppm) of protons in **MP2**.

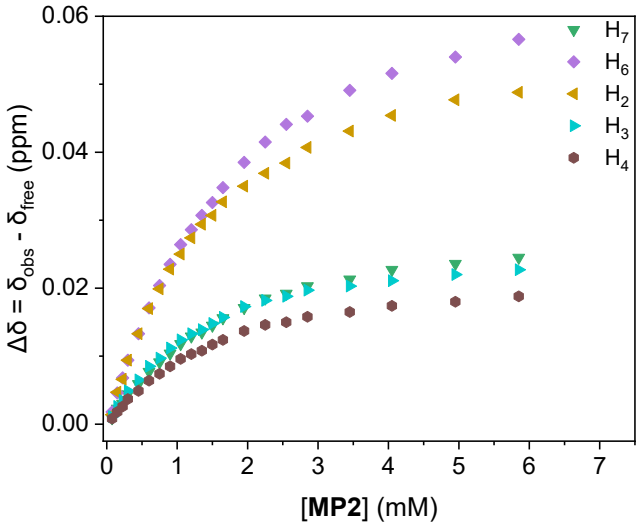

Figure S16. The observed ^{1}H NMR chemical shifts ($\Delta\delta = \delta_{observed} - \delta_{free}$, ppm) of protons in MC.

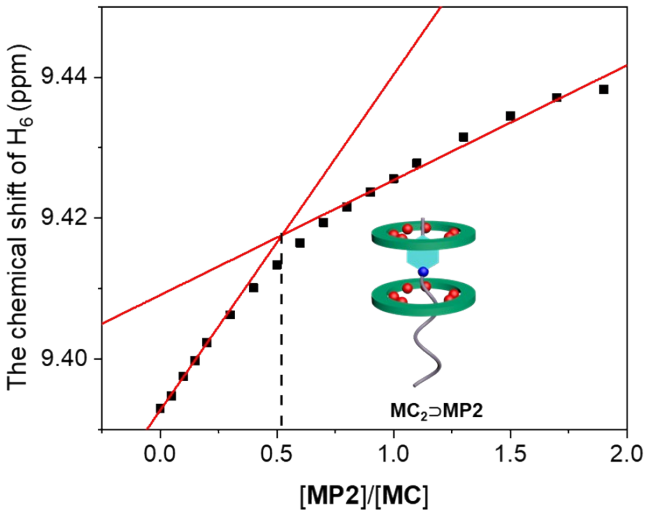

Figure S17. The mole ratio plot of the complexation of **MC** and **MP2** in $CDCl_3$/DMSO-d_6 = 4/1 at 298.0 K.

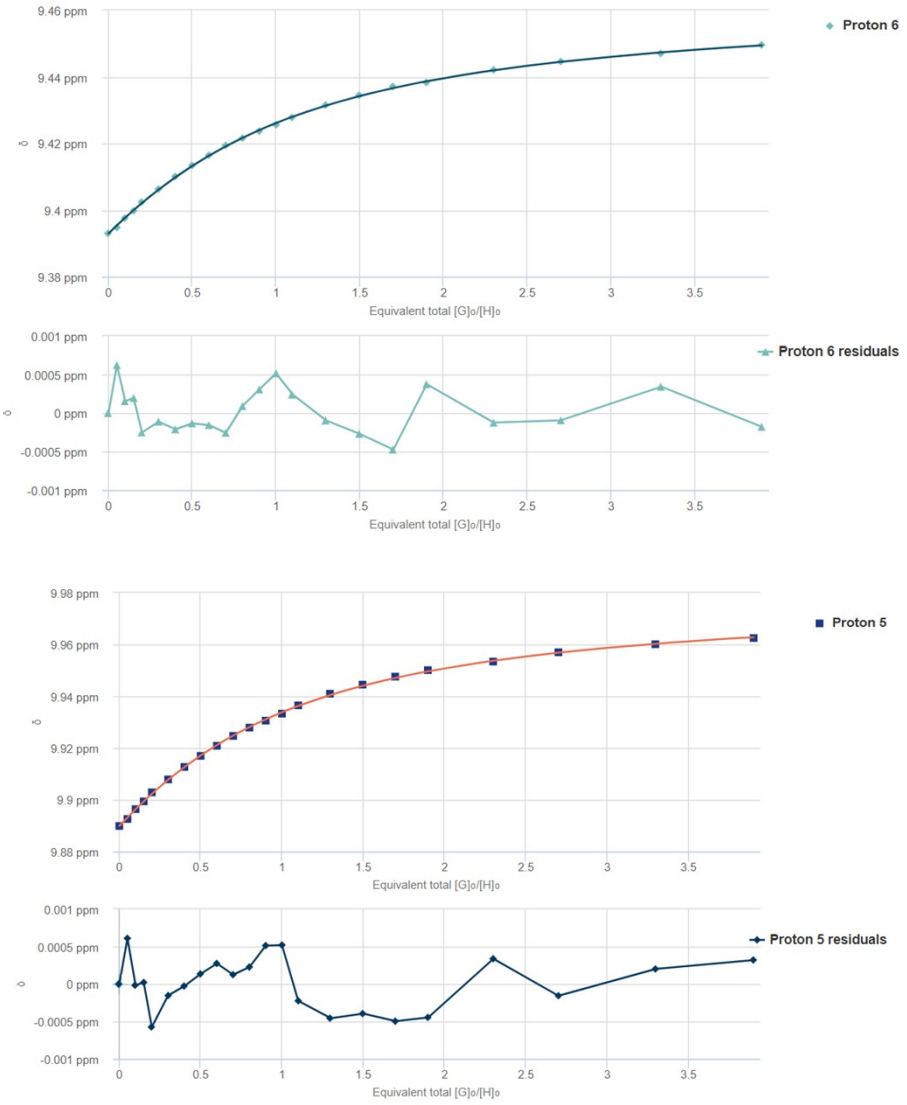

Details

Time to fit	1.2706 s
SSR	1.1142e-5
Fitted datapoints	132
Fitted params	14

Parameters

Parameter (bounds)	Optimised	Error	Initial
K_{11} (0 → ∞)	1073.68 M^{-1}	± 0.8980 %	1000.00 M^{-1}
K_{21} (0 → ∞)	228.98 M^{-1}	± 2.7412 %	100.00 M^{-1}

Back Next

Figure S18. Nonlinear least-squares analysis of the ^{1}H NMR binding data (**Figure S14**) corresponding to the formation of **MC_2⊃MP2** complexes. The data were fitted to a 2:1 (host : guest) binding model to give K_{11} = (1.07 ± 0.01) × 10^3 M^{-1} and K_{21} = (2.29 ± 0.06) × 10^2 M^{-1}. The residual distribution is shown below the binding isotherm. All solid lines were obtained from non-linear curve-fitting with the Nelder–Mead method to a 2 : 1 binding model using the http://supramolecular.org/ web applet.

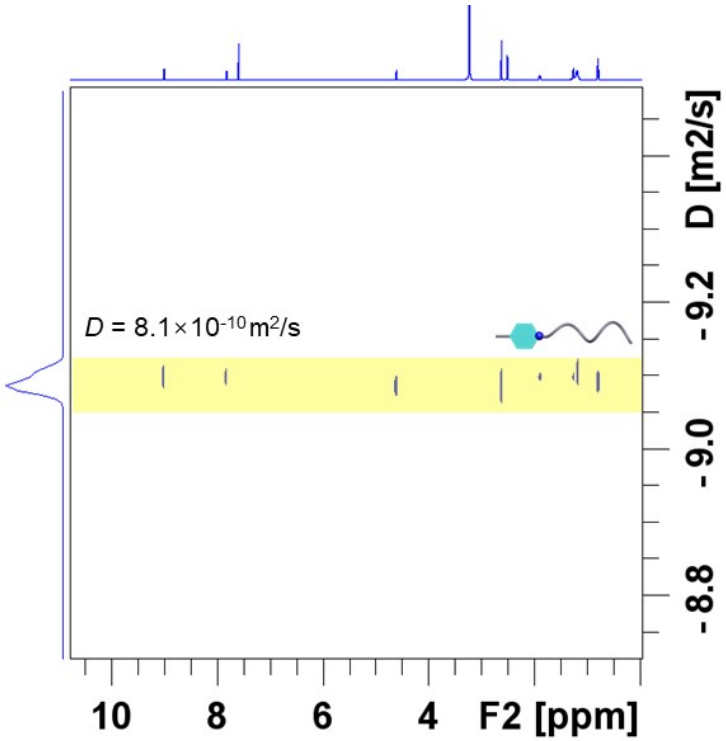

Figure S19. Partial DOSY spectrum (600 MHz, $CDCl_3$/DMSO-d_6 = 4/1, v/v, 298.0 K) of **MP2**. [**MP2**] = 1.0 mM.

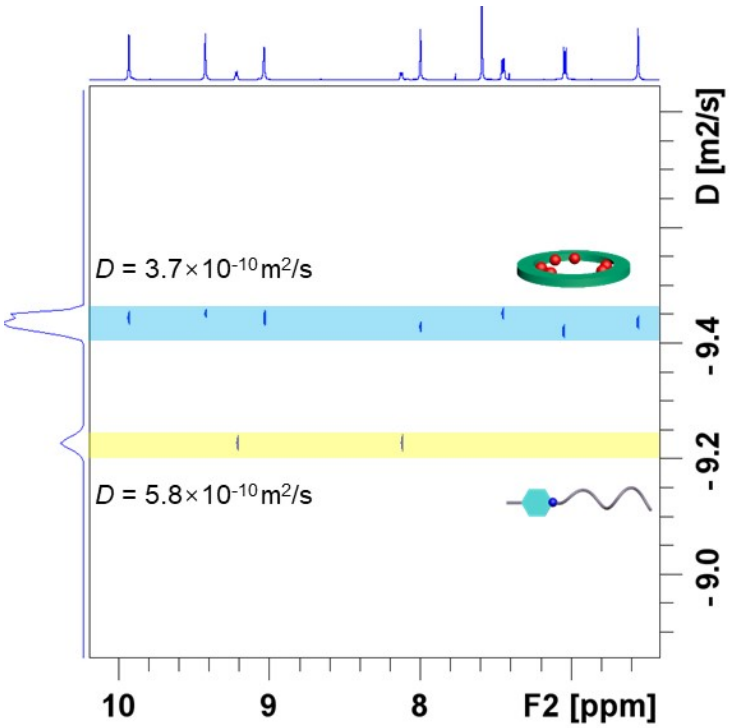

Figure S20. Partial DOSY spectrum (600 MHz, $CDCl_3$/DMSO-d_6 = 4/1, v/v, 298.0 K) of **MC_2⊃MP2**. [**MC**] = 2.0 mM, [**MP2**] = 1.0 mM.

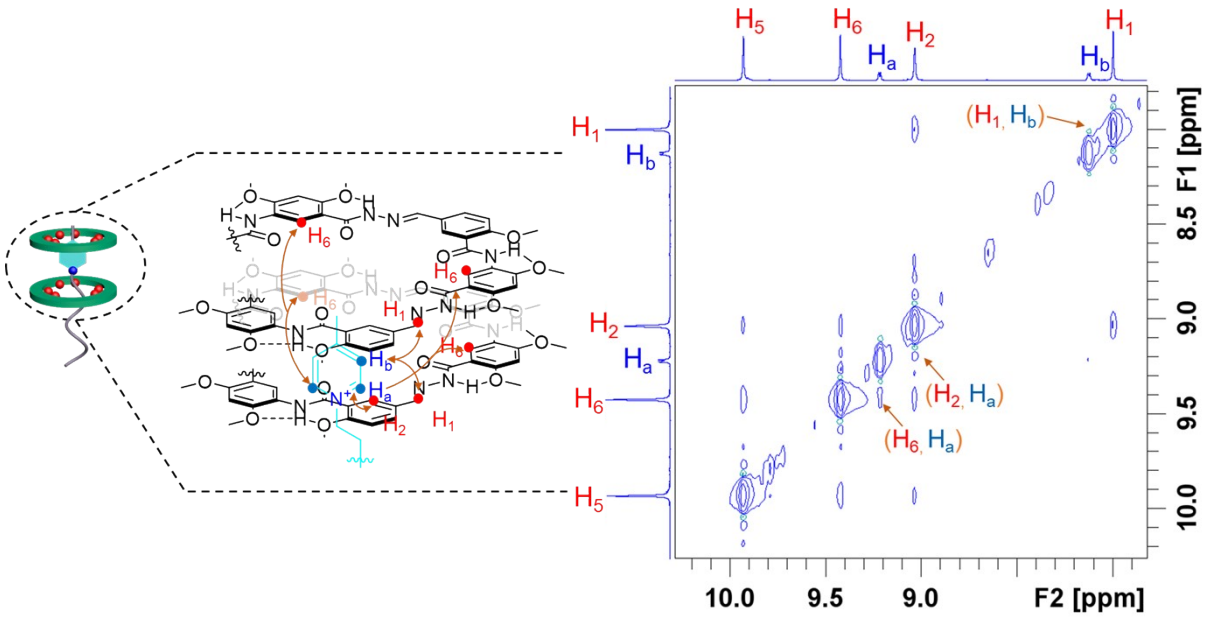

Figure S21. Partial **NOESY spectrum** (600 MHz, $CDCl_3$/DMSO-d_6 = 4/1, v/v, 298.0 K) of **MC_2⊃MP2**. [**MC**] = 2.0 mM, [**MP2**] = 1.0 mM. Arrows represent NOEs between **MC** and **MP2**. (The flexible alkyl chains were omitted for clarity.)

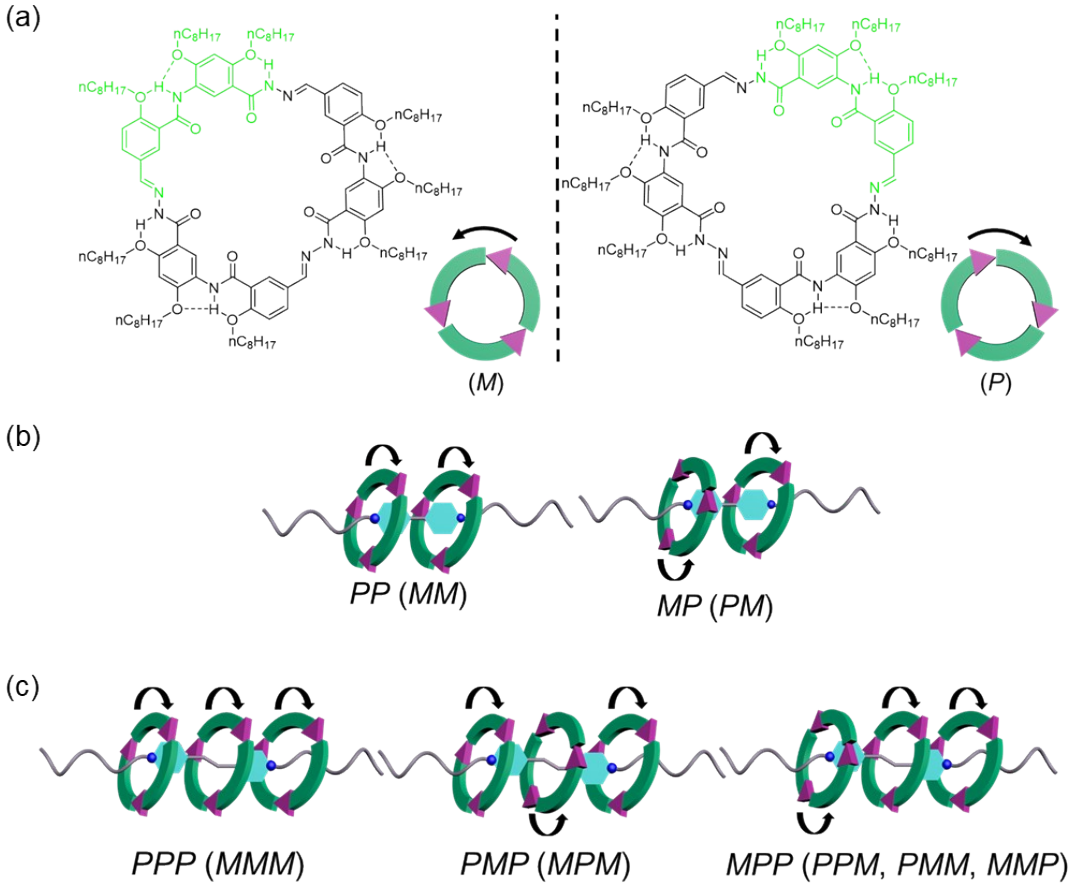

Figure S22. (a) Schematic illustration of macrocycle **MC** exhibits two rotational modes (*P* or *M*). Two types of [3]pseudorotaxane **MC_2⊃BP1** (b) and three types of [3]pseudorotaxane **MC_3⊃BP2** (c) were generated by combining macrocycle **MC** of different orientations respectively.

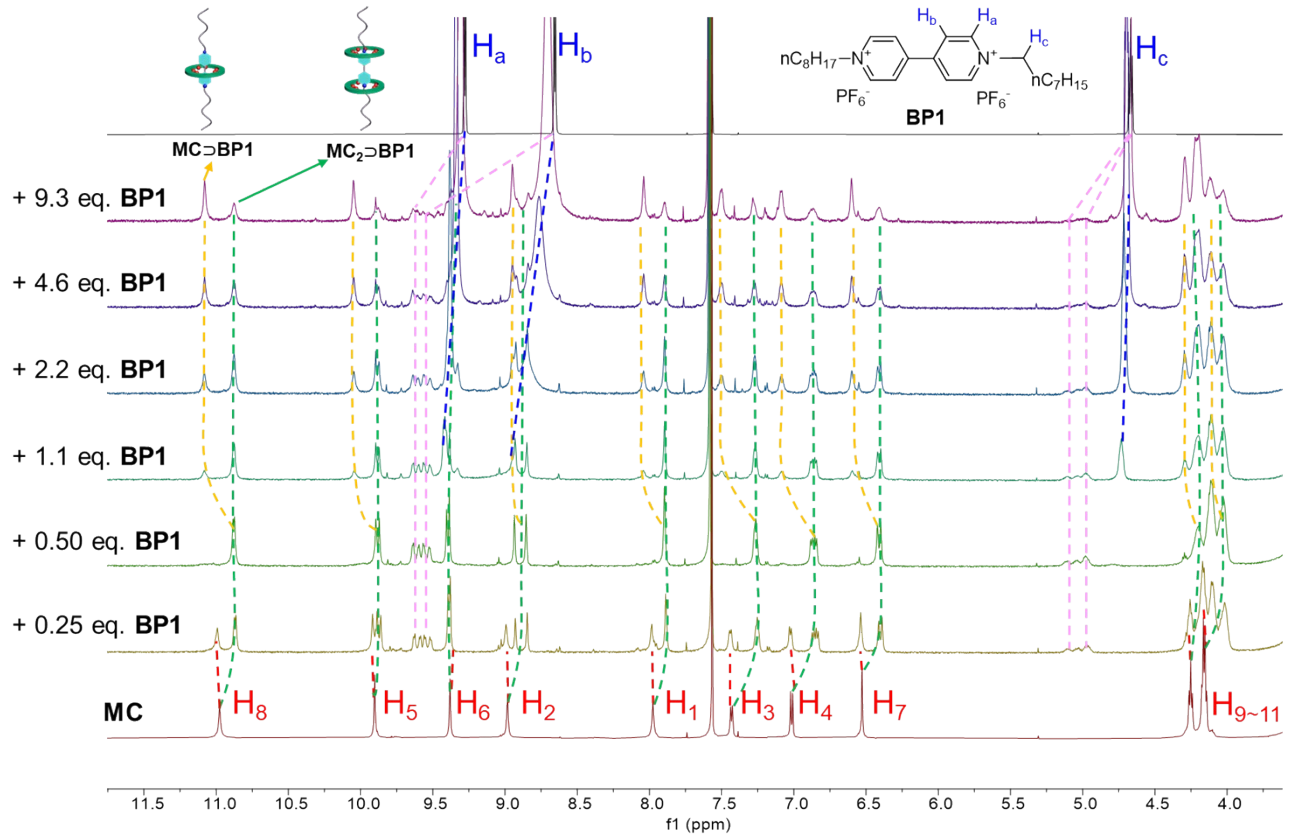

Figure S23. Partial ^{1}H NMR spectra (600 MHz, $CDCl_3$/DMSO-d_6 = 4/1, v/v, 298.0 K) of **MC** at a concentration of 1.0 mM with different equivalent of **BP1** (The pink dotted line represents the bound guest, the blue dotted line represents the free guest).

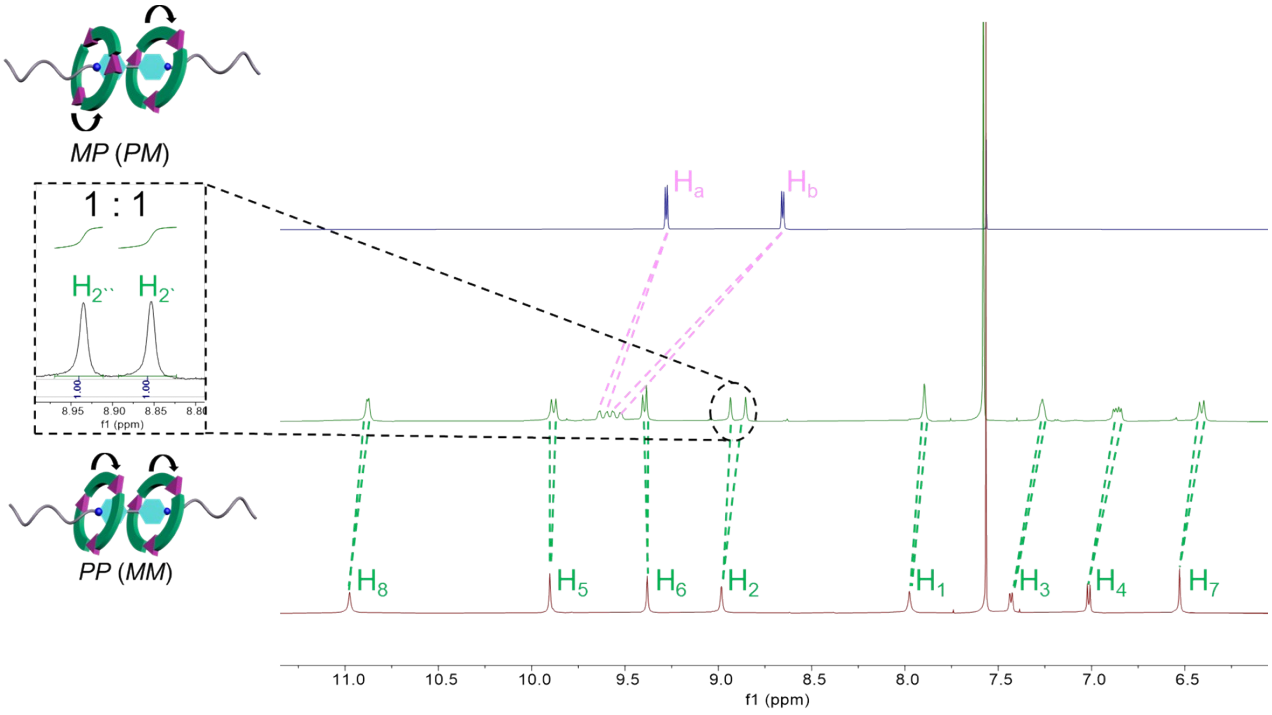

Figure S24. Partial ^{1}H NMR spectra (600 MHz, $CDCl_3$/DMSO-d_6 = 4/1, v/v, 298.0 K) of **MC$_2$⊃BP1**. [**MC**] = 2.0 mM, [**BP1**] = 1.0 mM.

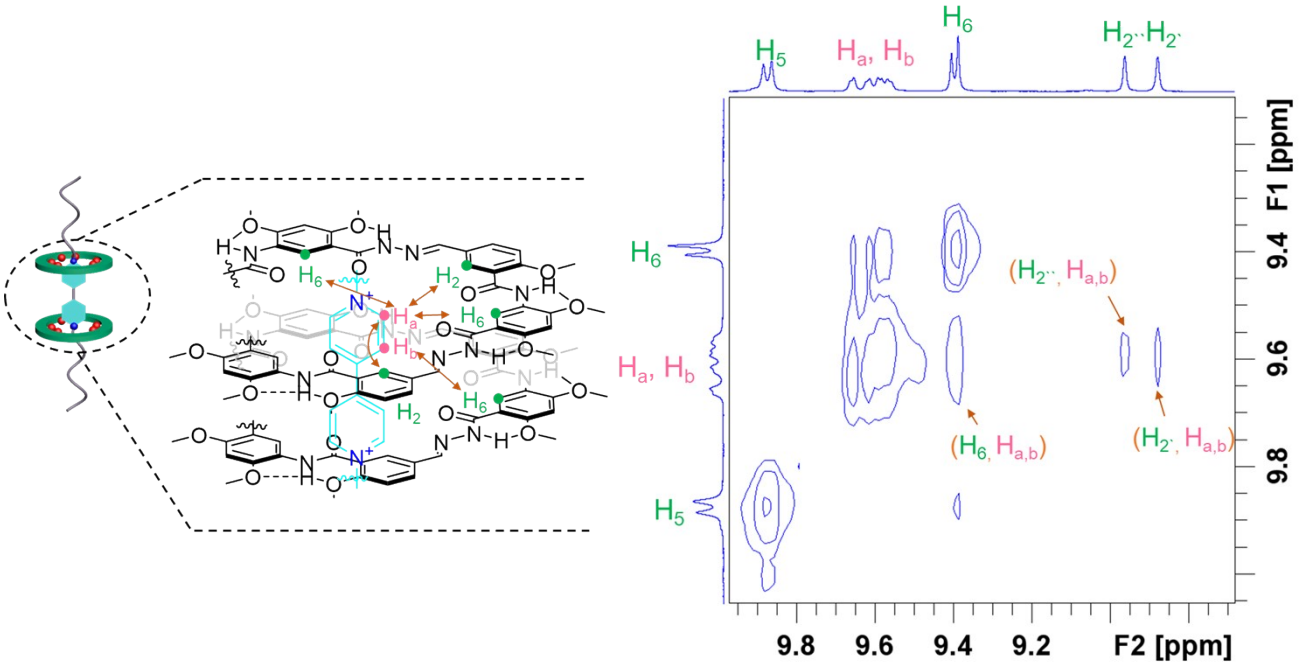

Figure S25. Partial **NOESY spectrum** (600 MHz, $CDCl_3$/DMSO-d_6 = 4/1, v/v, 298.0 K) of **MC**$_2$⊃**BP1**. [**MC**] = 2.0 mM, [**BP1**] = 1.0 mM. Arrows represent NOEs between **MC** and **BP1**. (The flexible alkyl chains were omitted for clarity.)

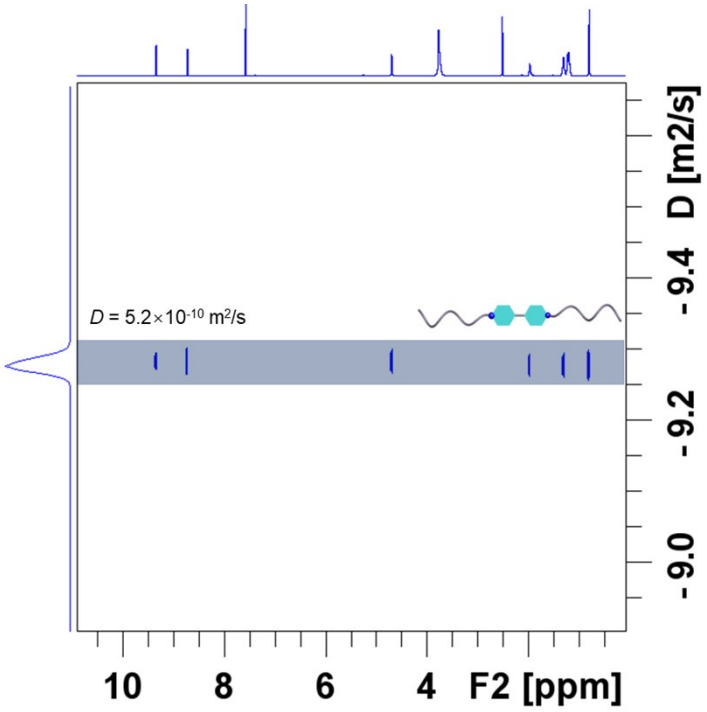

Figure S26. Partial DOSY spectrum (600 MHz, $CDCl_3$/DMSO-d_6 = 4/1, v/v, 298.0 K) of **BP1**. [**BP1**] = 1.0 mM.

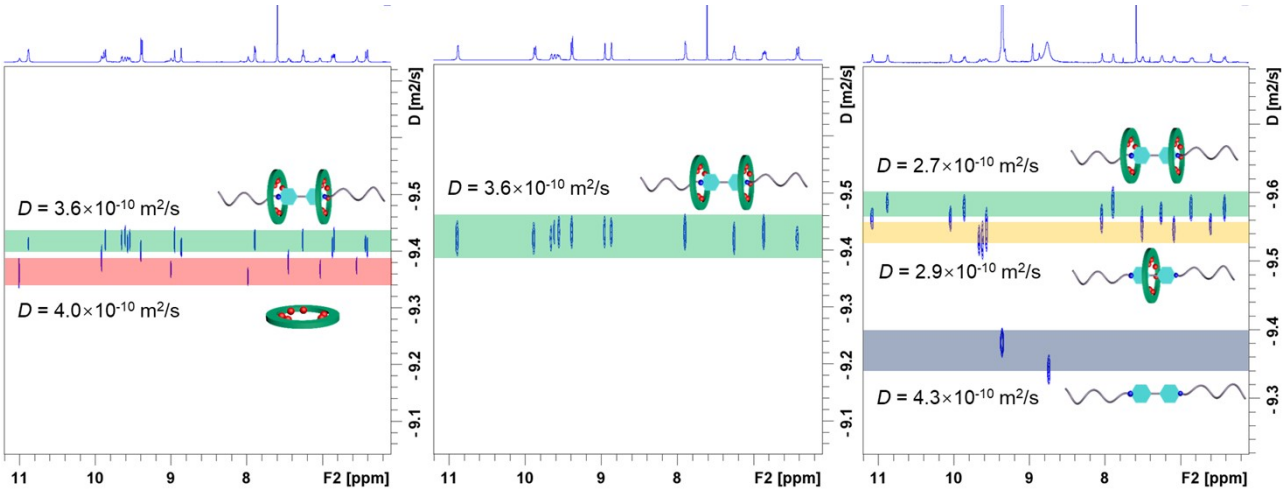

Figure S27. Partial DOSY spectra (600 MHz, $CDCl_3$/DMSO-d_6 = 4/1, v/v, 298.0 K) of **MC** with 0.25 eq. (left), 0.50 eq. (middle), 4.6 eq. (right) **BP1**. [**MC**] = 1.0 mM.

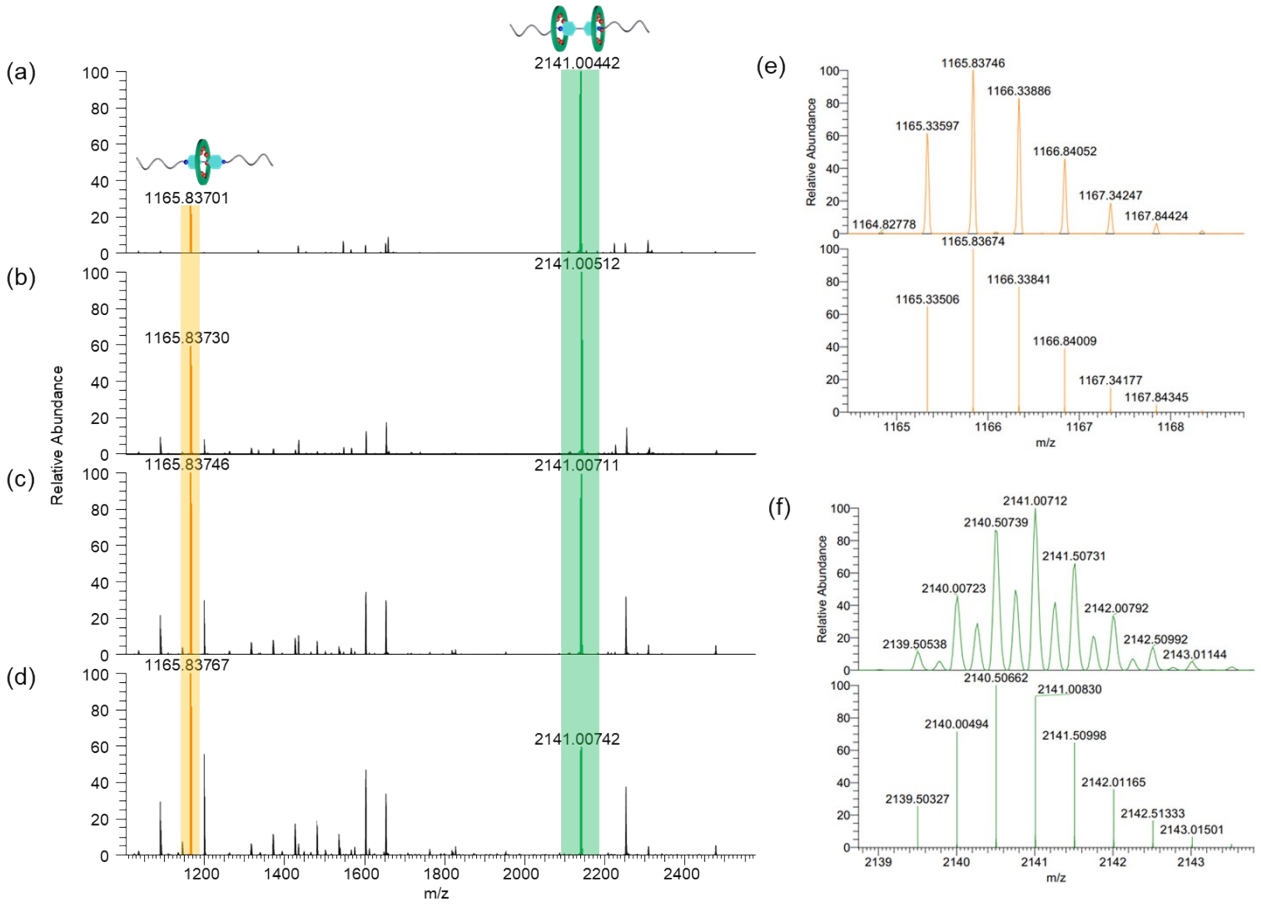

Figure S28. ESI mass spectra of **MC** with (a) 1.1 eq., (b) 3.2 eq., (c)7.6 eq. and (d)13 eq. **BP1**, ESI mass spectra of (e) **MC⊃BP1** and (**f**) **MC_2⊃BP1** (top: experimental, bottom: simulated).

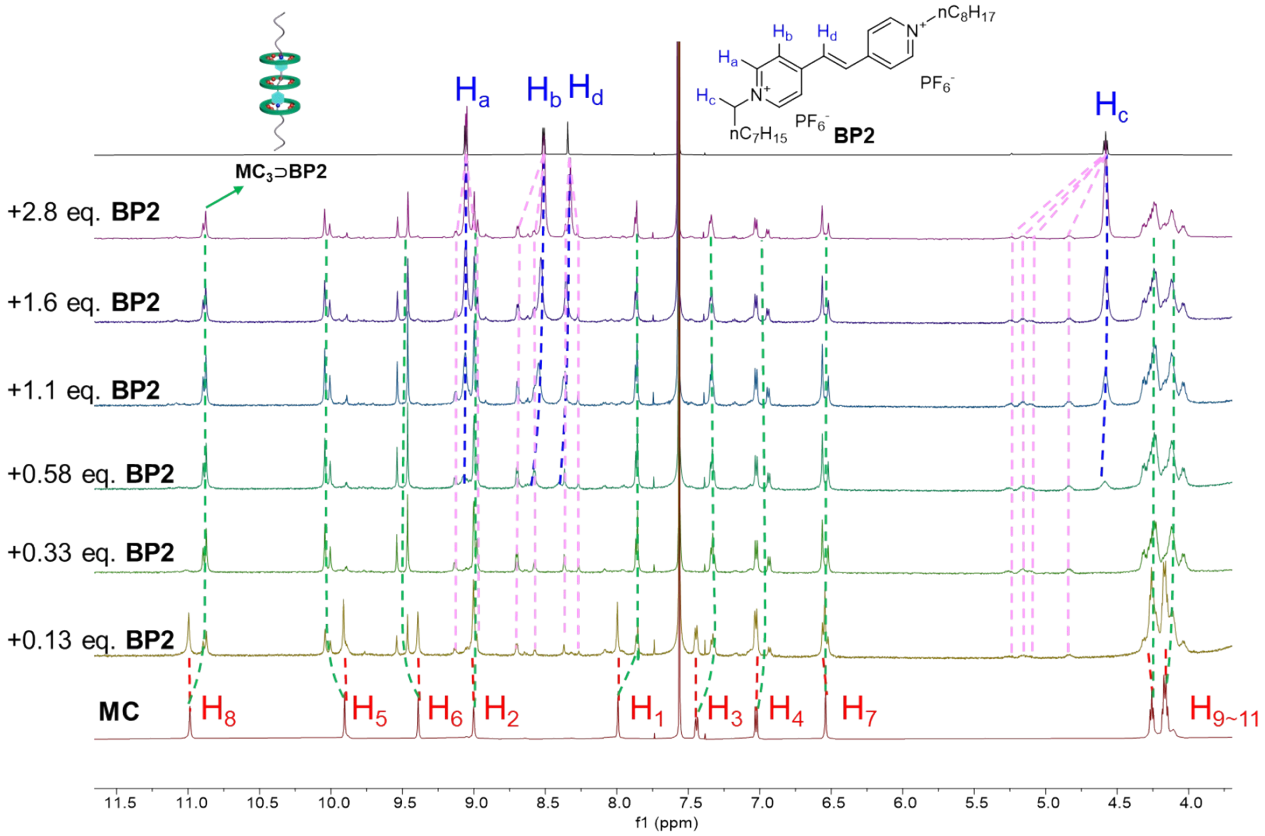

Figure S29. Partial ^{1}H NMR spectra (600 MHz, $CDCl_3$/DMSO-d_6 = 4/1, v/v, 298.0 K) of **MC** at a concentration of 1.0 mM with different equivalent of **BP2** (The pink dotted line represents the bound guest, the blue dotted line represents the free guest).

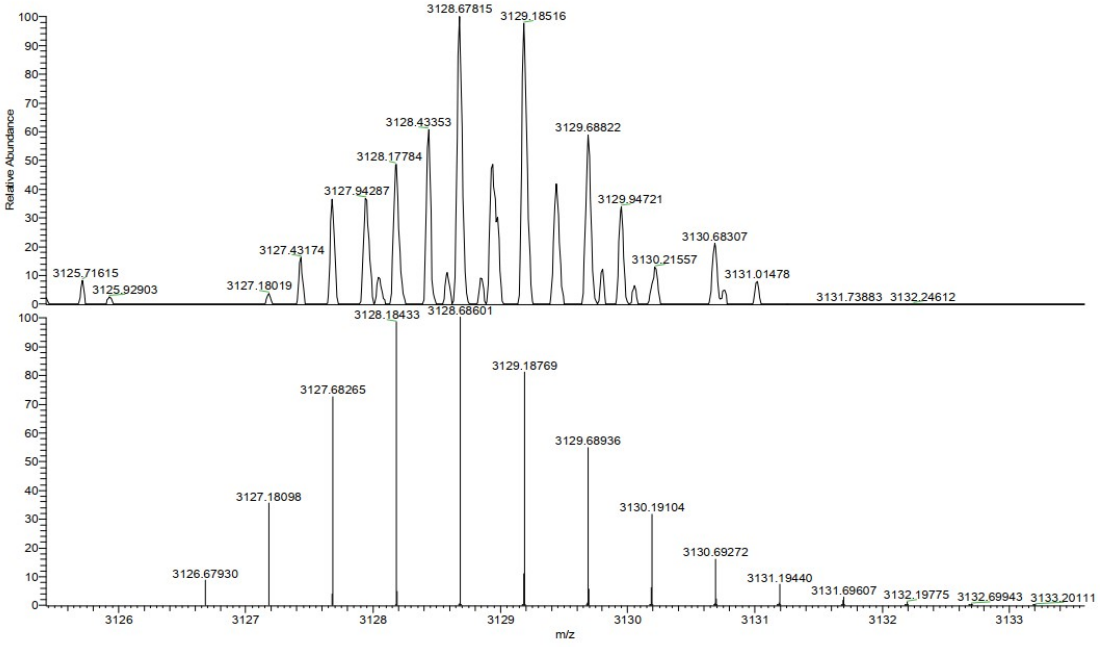

Figure S30. ESI mass spectra of **MC$_3$⊃BP2** (top: experimental, bottom: simulated).

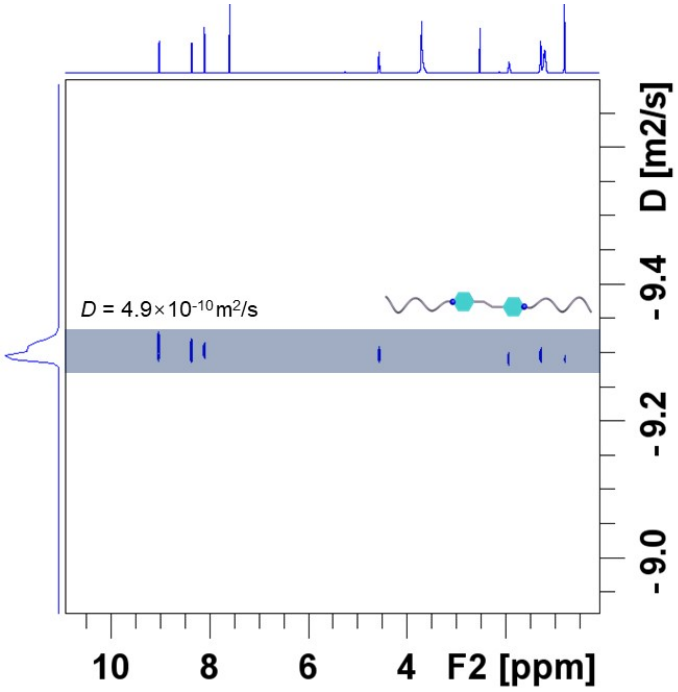

Figure S31. Partial DOSY spectrum (600 MHz, $CDCl_3$/DMSO-d_6 = 4/1, v/v, 298.0 K) of **BP2**. [**BP2**] = 1.0 mM.

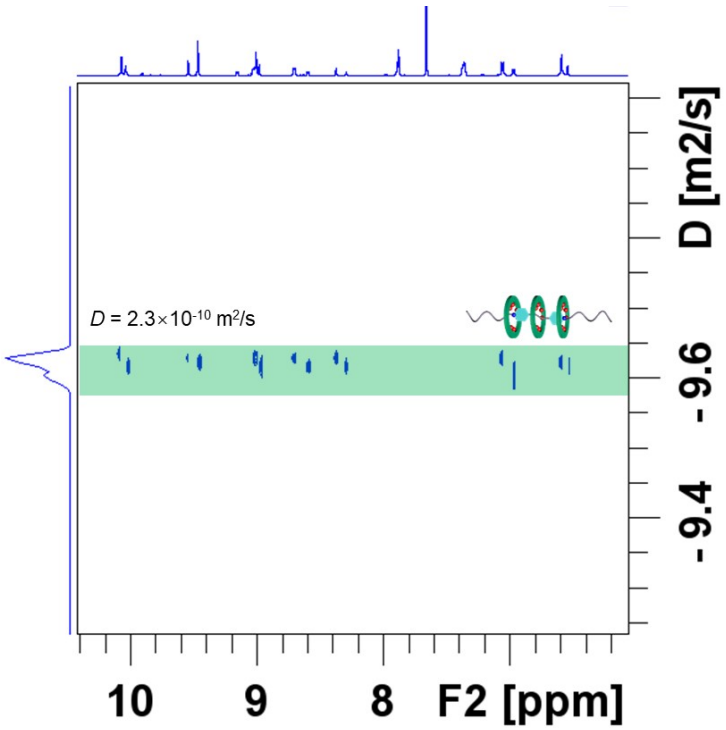

Figure S32. Partial DOSY spectrum (600 MHz, $CDCl_3$/DMSO-d_6 = 4/1, v/v, 298.0 K) of **MC_3⊃BP2**. [**MC**] = 3.0 mM, [**BP2**] = 1.0 mM.

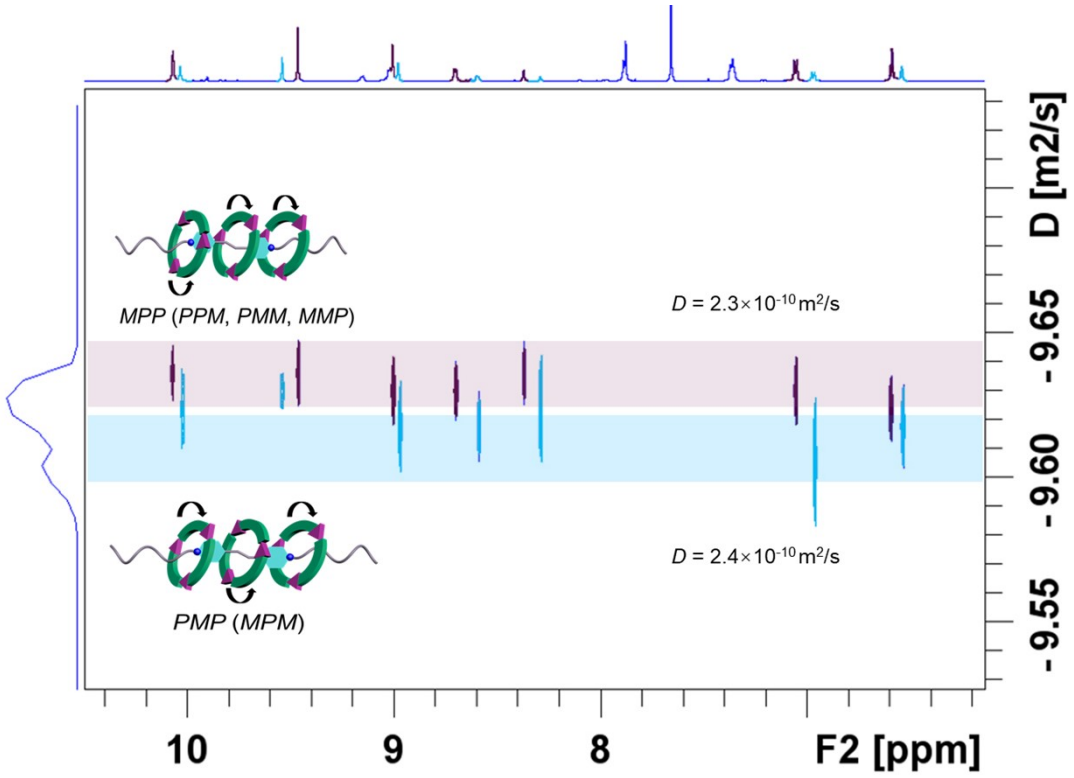

Figure S33. Partial DOSY spectrum (600 MHz, $CDCl_3$/DMSO-d_6 = 4/1, v/v, 298.0 K) of *MPP* (*PPM*, *PMM*, *MMP*) and *PMP* (*MPM*). [**MC**] = 3.0 mM, [**BP2**] = 1.0 mM.

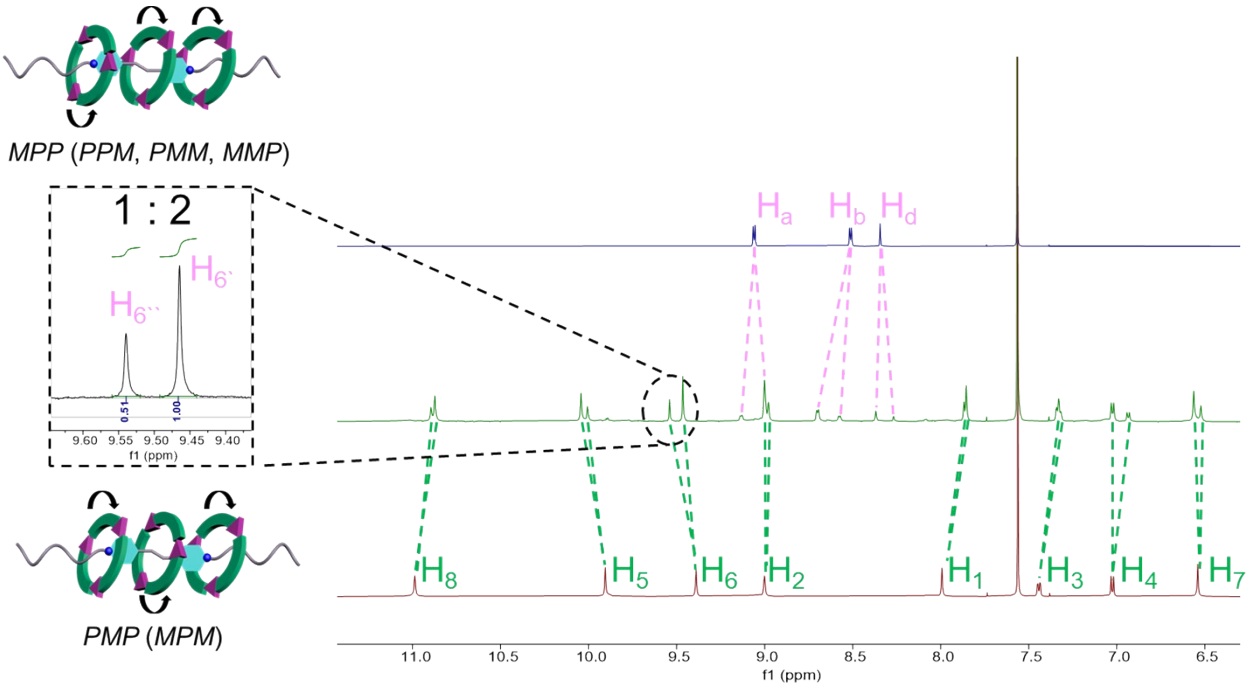

Figure S34. Partial ^{1}H NMR spectra (600 MHz, $CDCl_3$/DMSO-d_6 = 4/1, v/v, 298.0 K) of **MC$_3$⊃BP2**. [**MC**] = 3.0 mM, [**BP2**] = 1.0 mM.

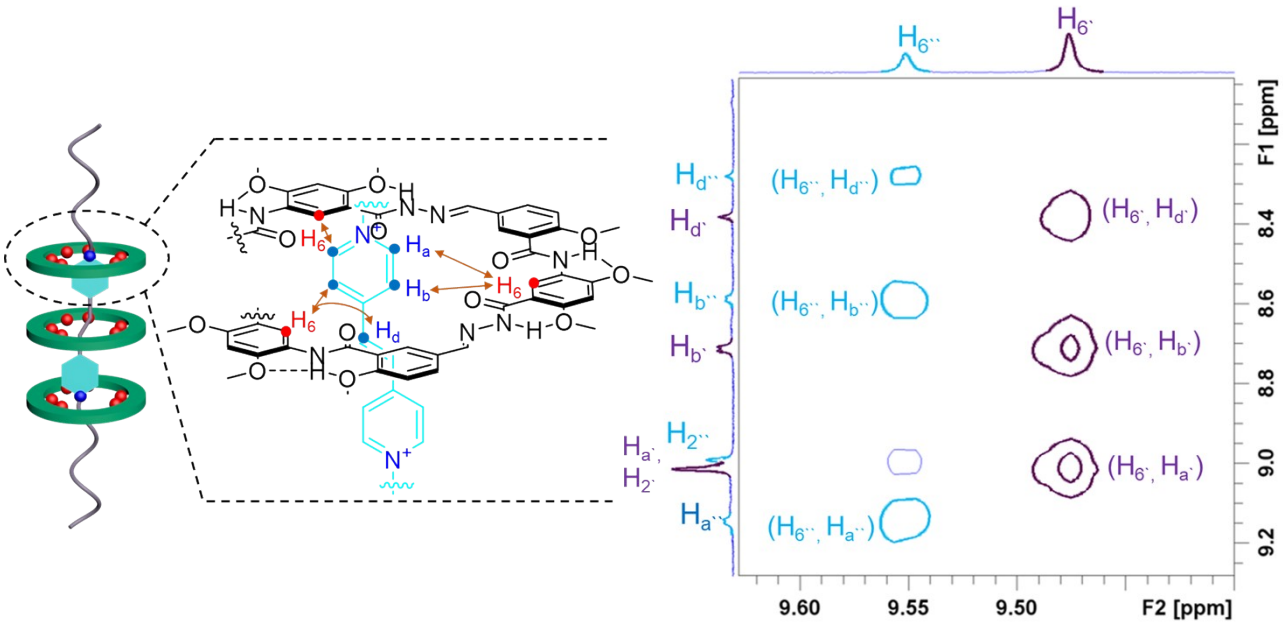

Figure S35. Partial NOESY spectrum (600 MHz, $CDCl_3$/DMSO-d_6 = 4/1, v/v, 298.0 K) of **MC$_3$⊃BP2**. [**MC**] = 3.0 mM, [**BP2**] = 1.0 mM.

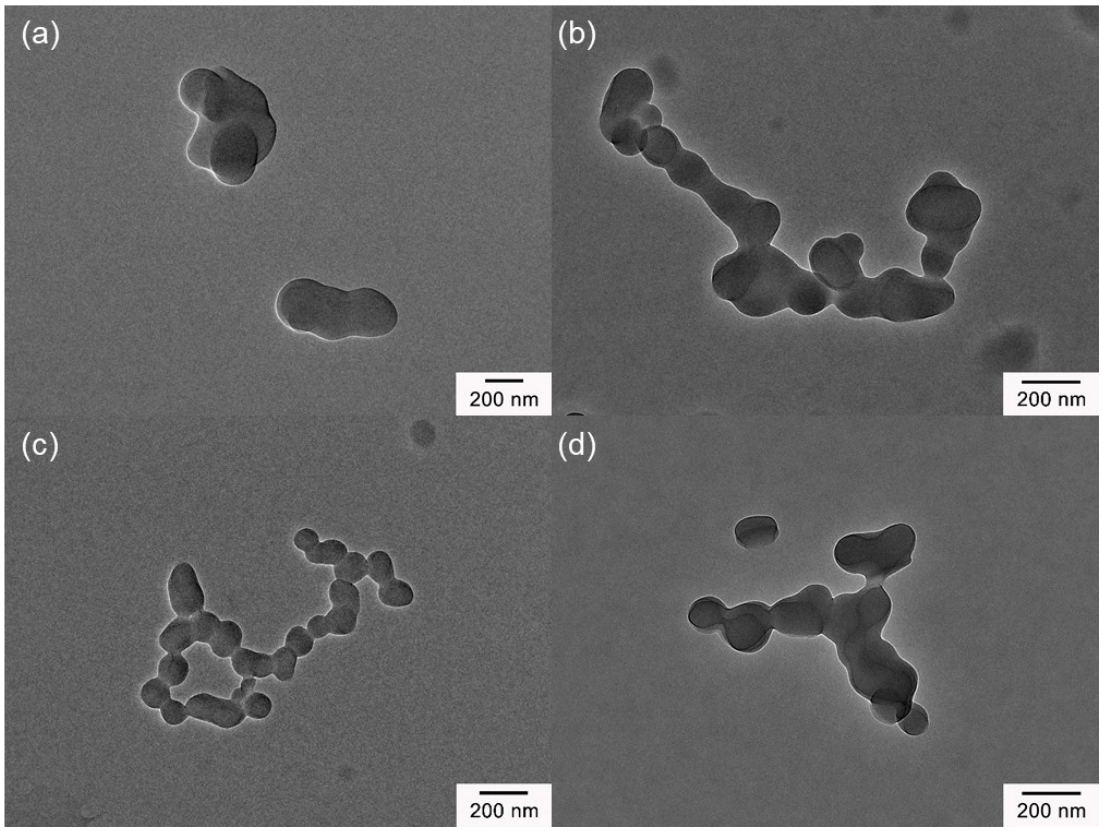

Figure S36. TEM images of the guests (a) **MP1**, (b) **MP2**, (c) **BP1** and (d) **BP2**.

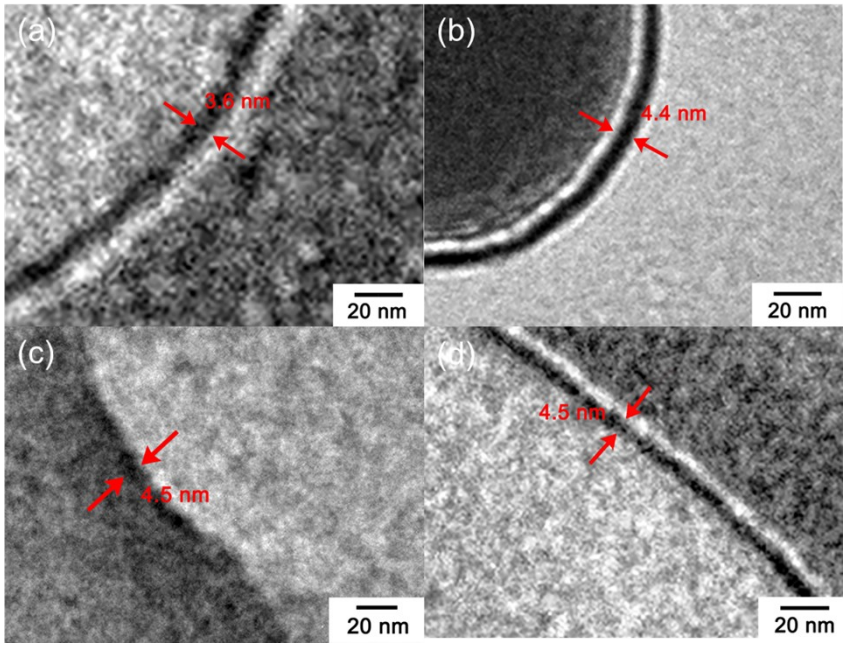

Figure S37. TEM images of the thick membrane of (a) vesicle [**MC$_2$⊃MP1**], (b) vesicle [**MC$_2$⊃MP2**], (c) vesicle [**MC$_2$⊃BP1**] and (d) vesicle [**MC$_3$⊃BP2**]. (TEM image of [**MC$_2$⊃BP1**] stained with uranyl acetate).

^{1}H, ^{13}C and HR-MS spectra for guests

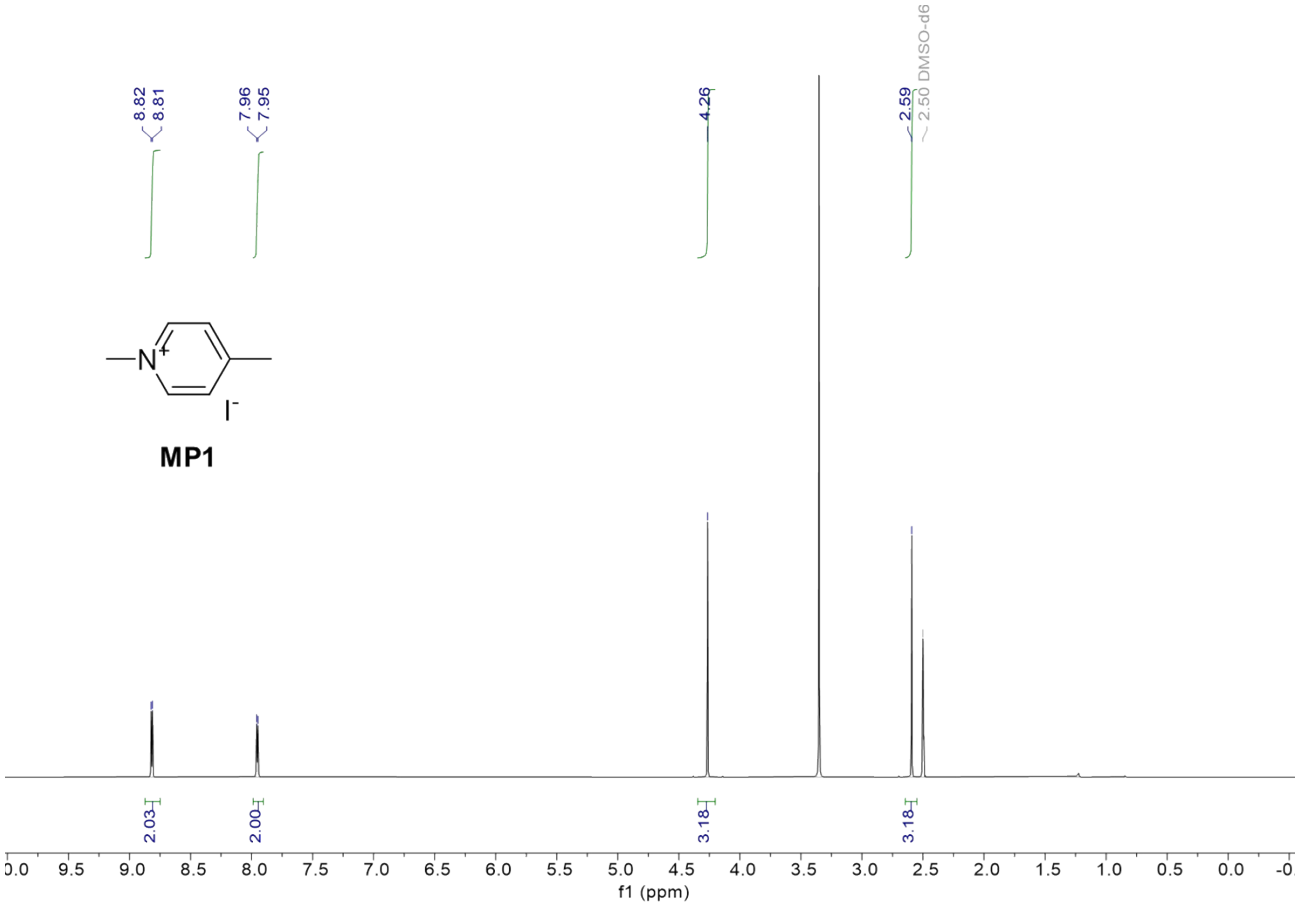

^{1}H NMR spectrum (600 MHz, DMSO-d_6, 298.0 K) of guest **MP1**.

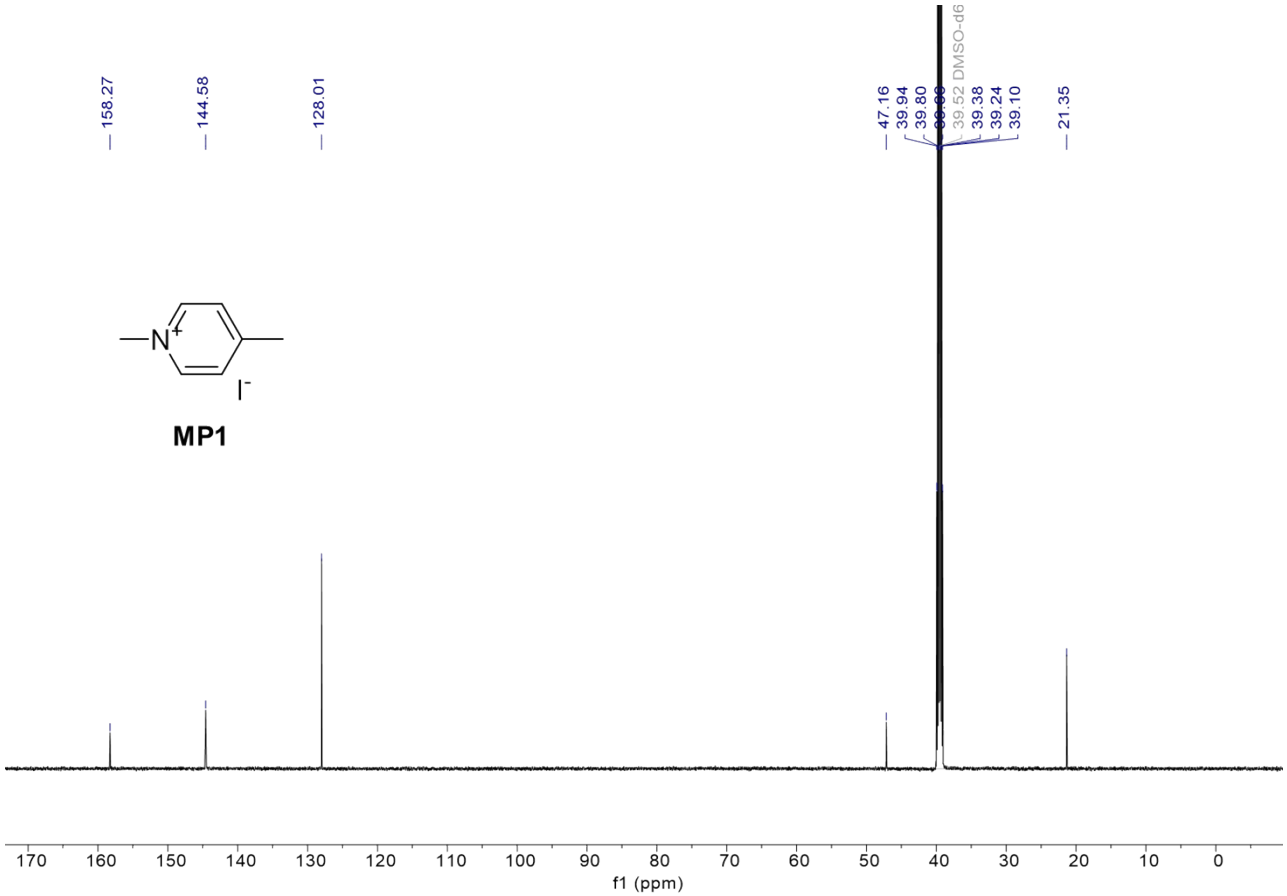

^{13}C NMR spectrum (150 MHz, DMSO-d_6, 298.0 K) of guest **MP1**.

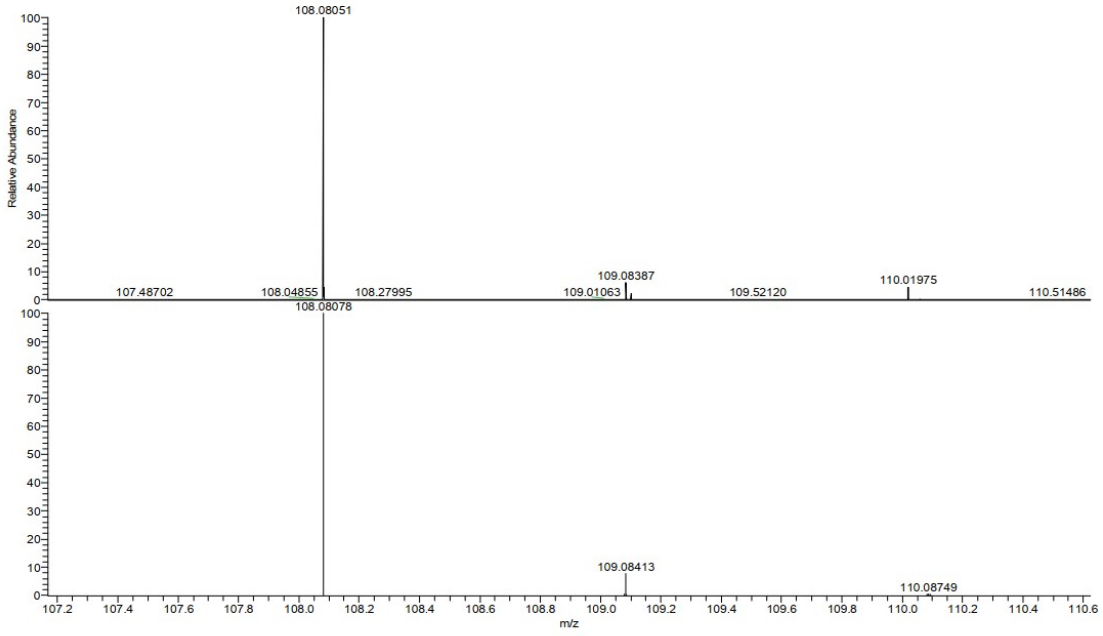

HRMS (ESI)-mass spectrum of guest **MP1**.

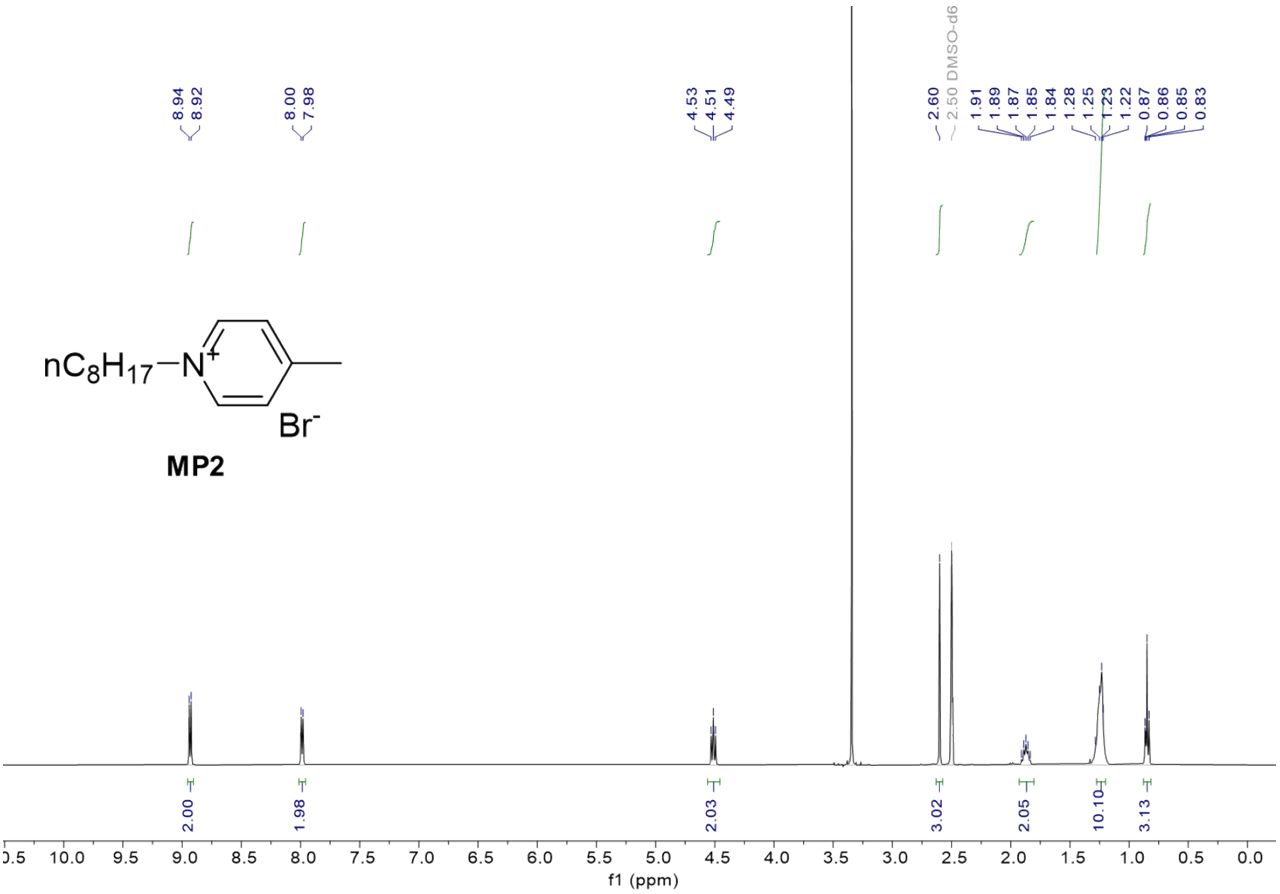

^{1}H NMR spectrum (600 MHz, DMSO-d_6, 298.0 K) of guest **MP2**.

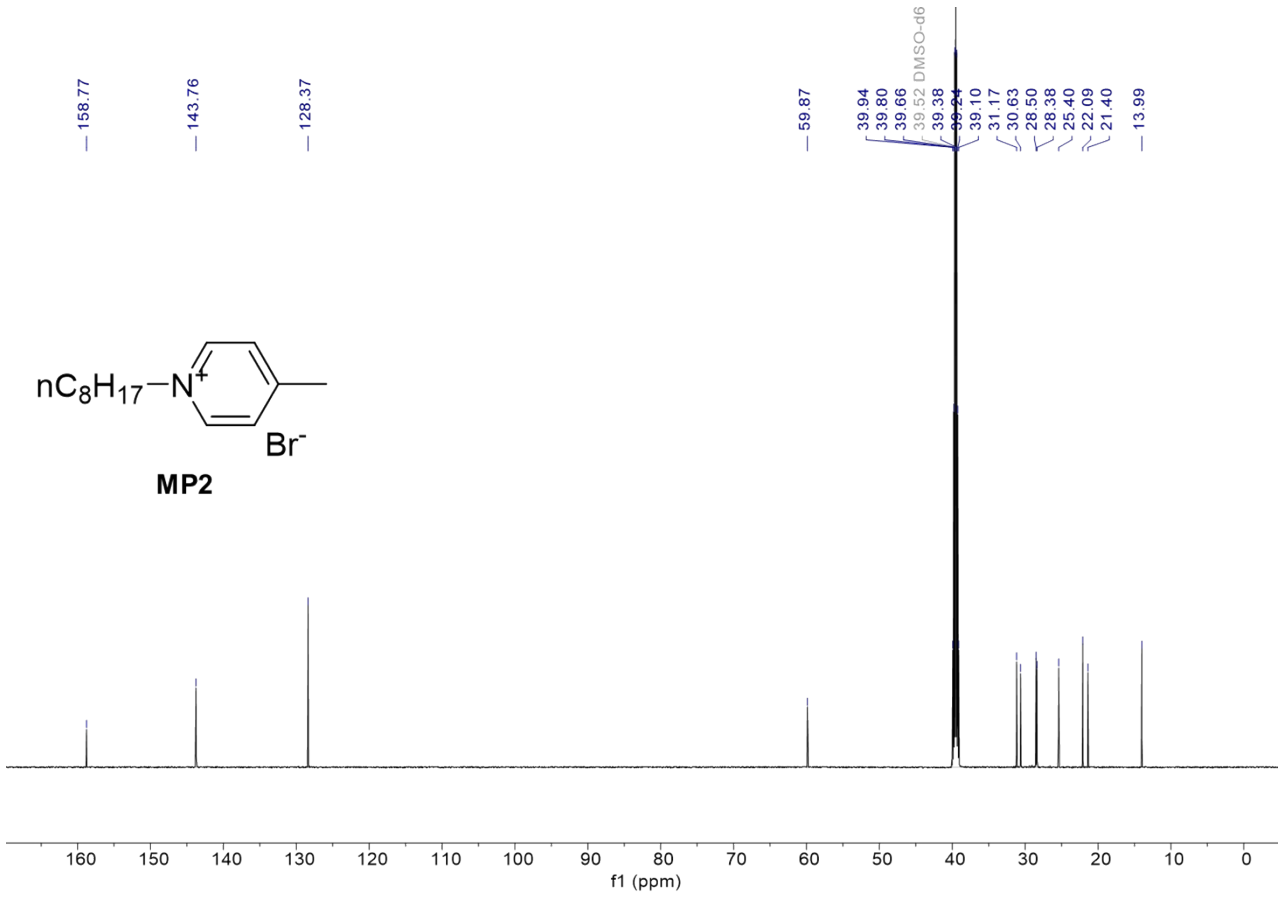

^{13}C NMR spectrum (150 MHz, DMSO-d_6, 298.0 K) of guest **MP2**.

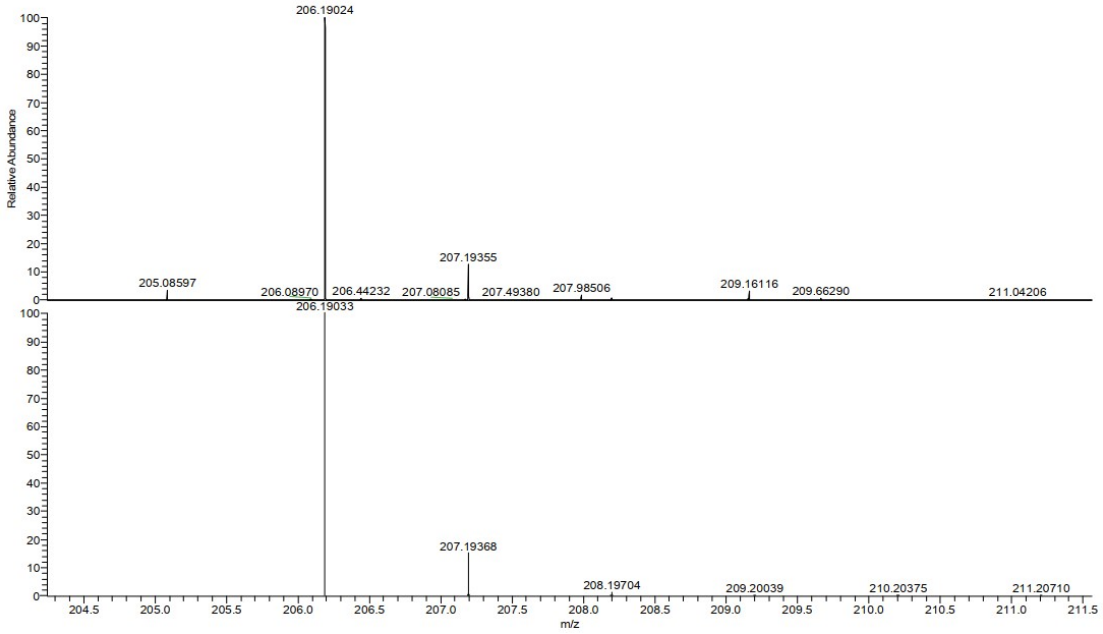

HRMS (ESI)-mass spectrum of guest **MP2**.

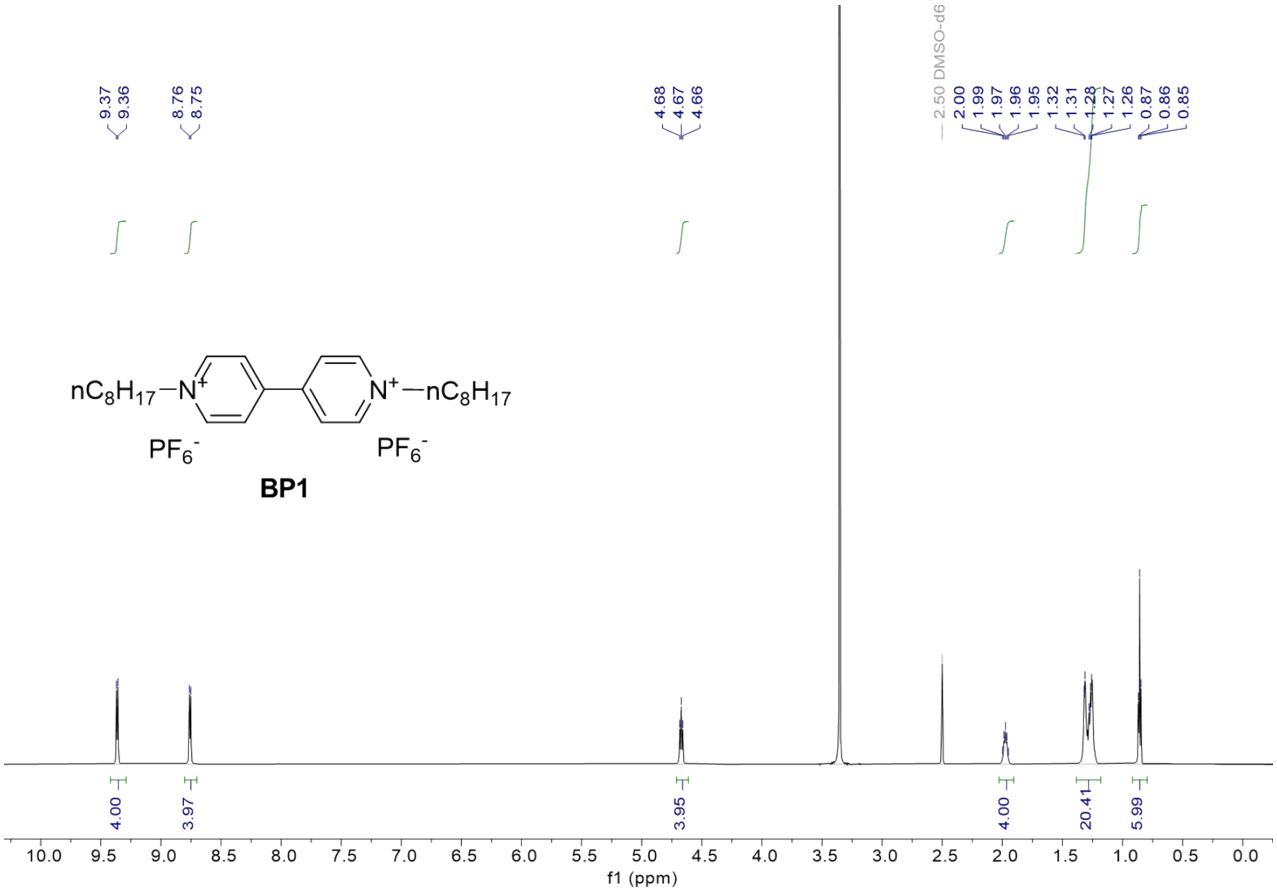

^{1}H NMR spectrum (600 MHz, DMSO-d_6, 298.0 K) of guest **BP1**

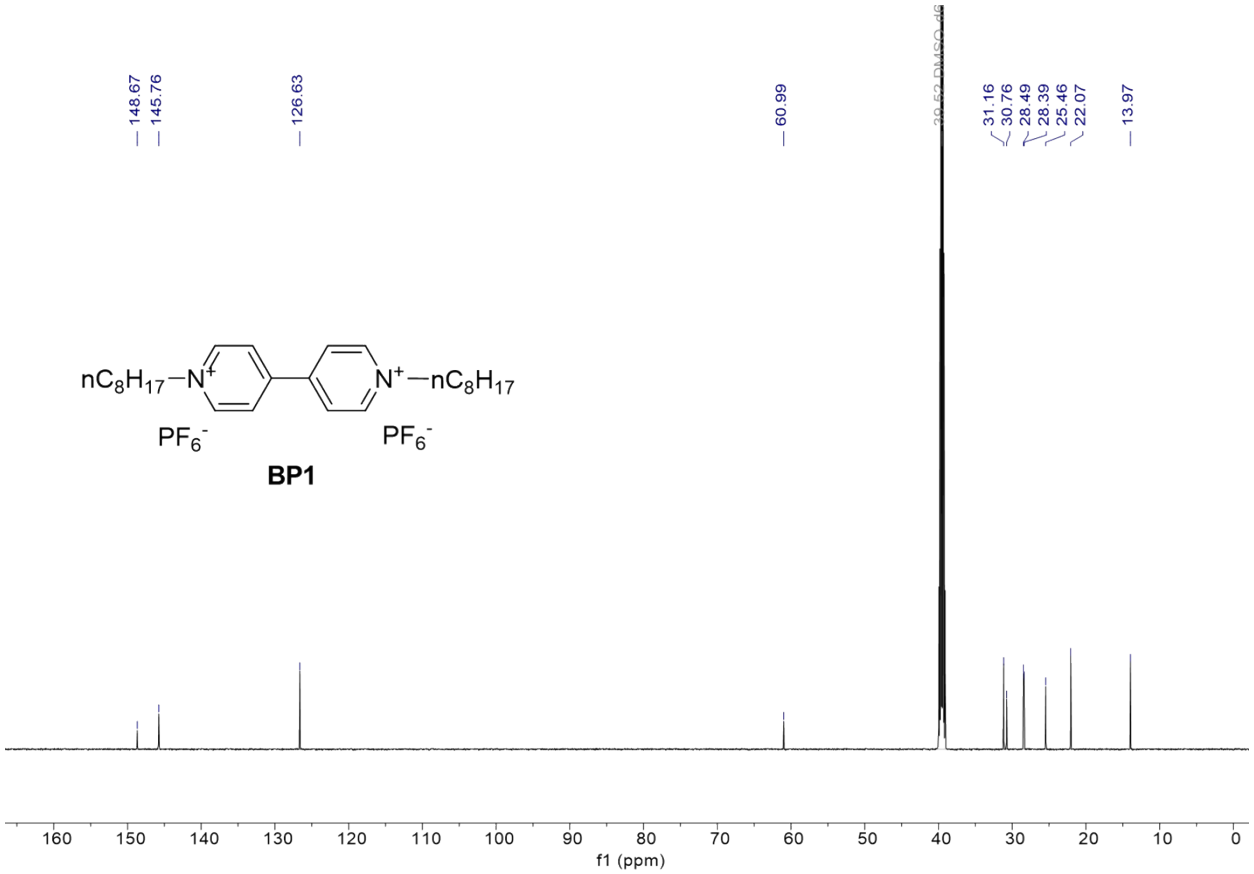

^{13}C NMR spectrum (150 MHz, DMSO-d_6, 298.0 K) of guest **BP1**.

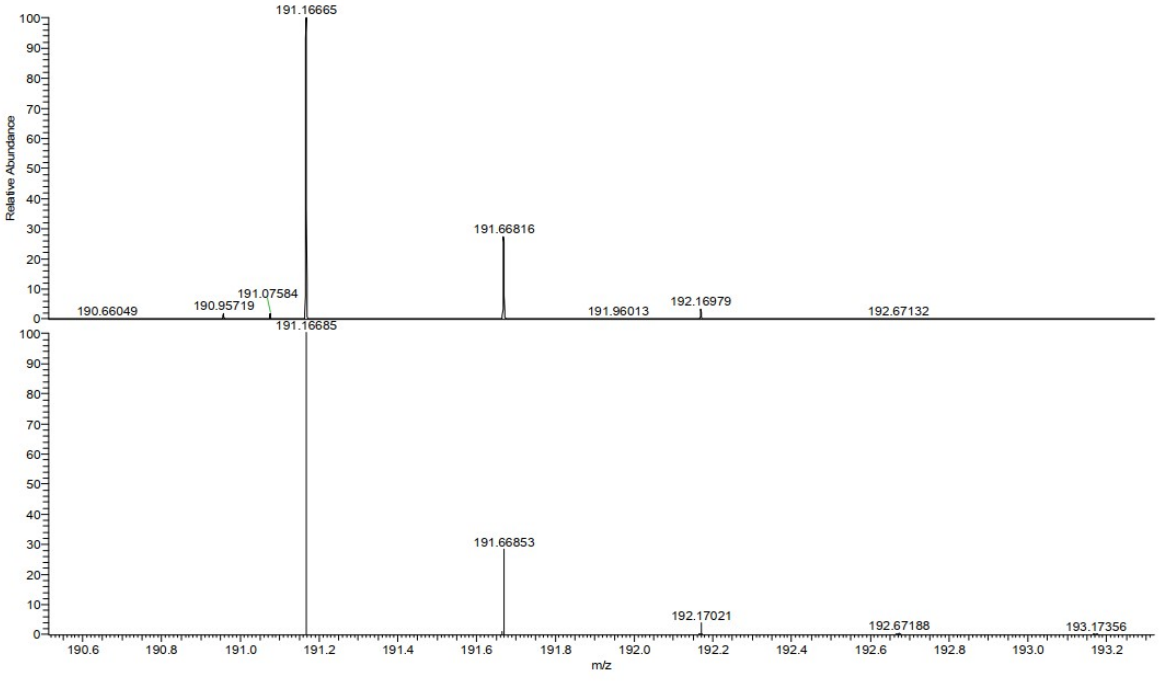

HRMS (ESI)-mass spectrum of guest **BP1**.

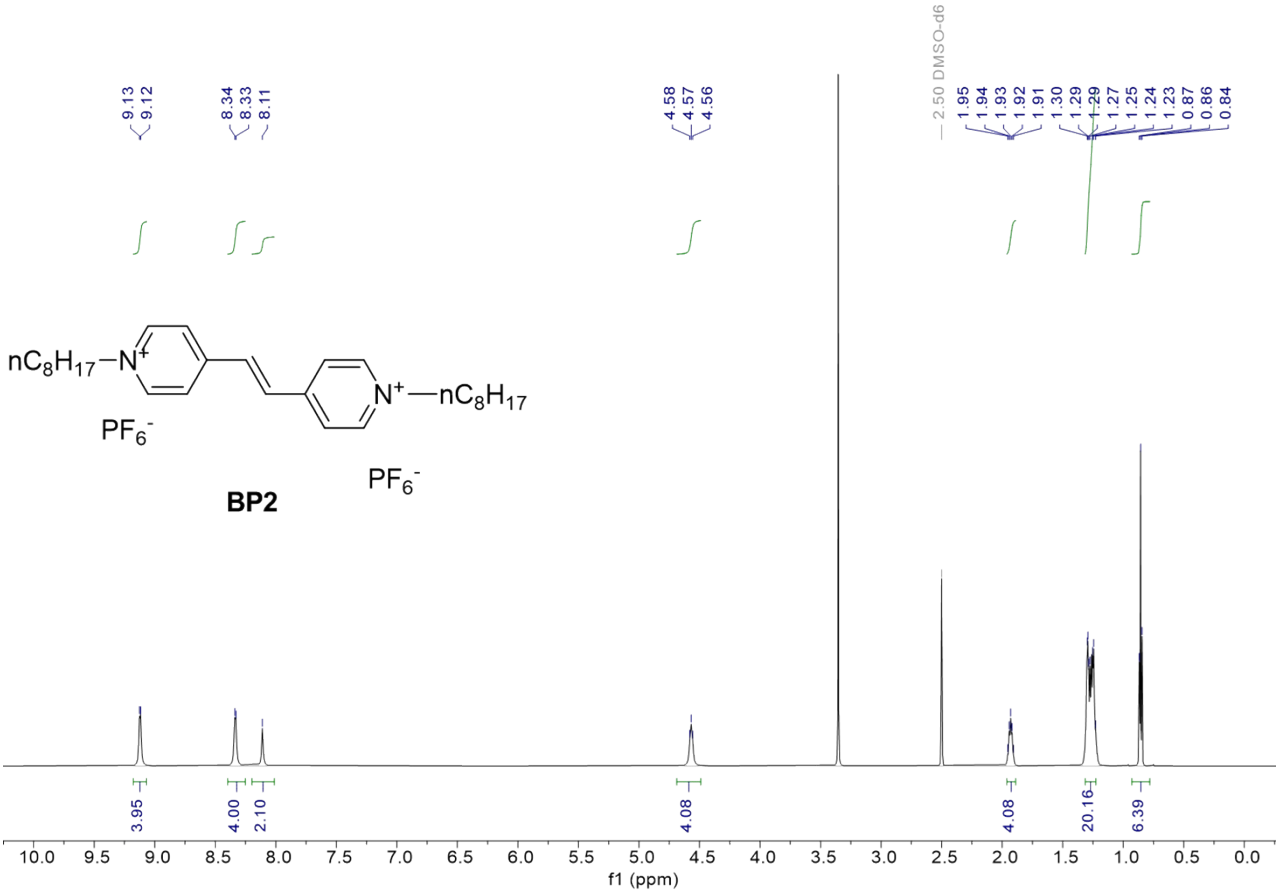

^{1}H NMR spectrum (600 MHz, DMSO-d_6, 298.0 K) of guest **BP2.**

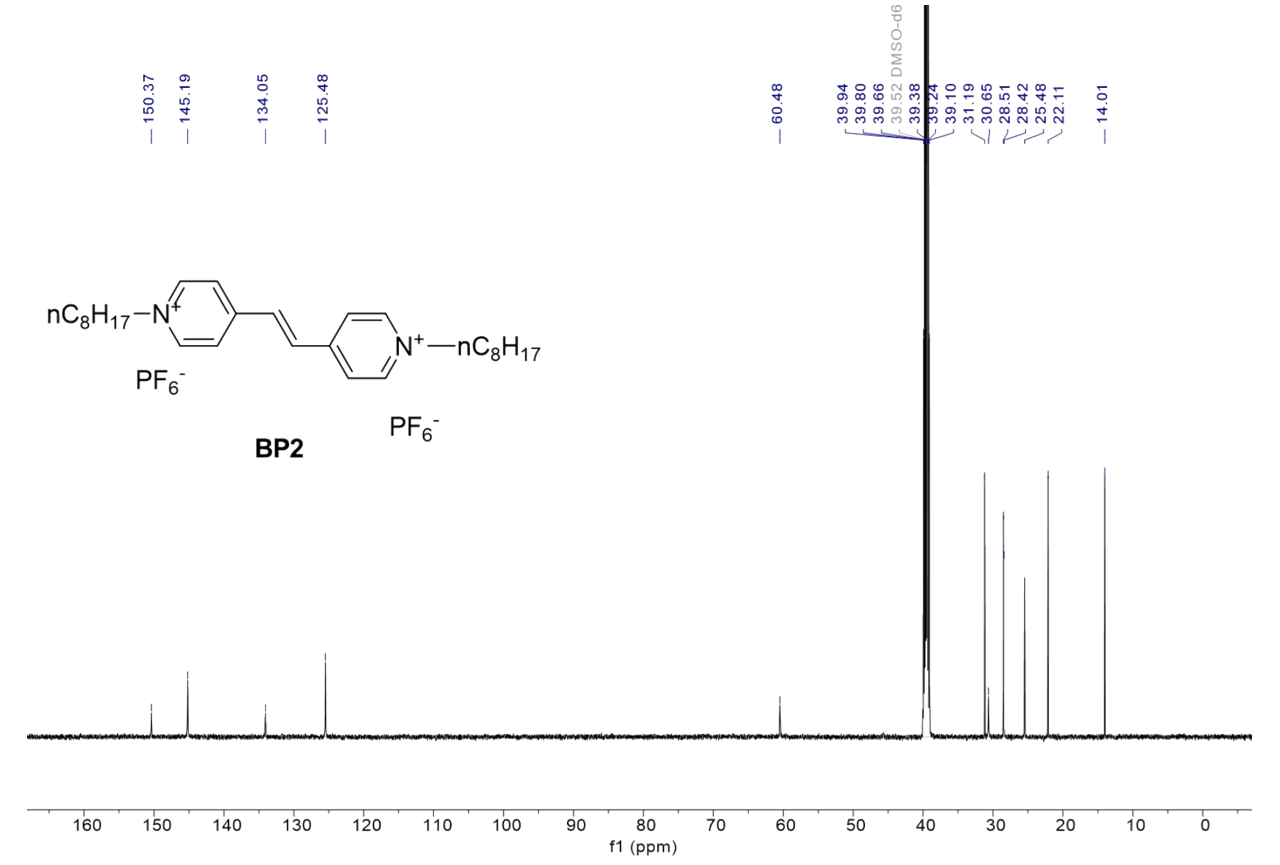

^{13}C NMR spectrum (150 MHz, DMSO-d_6, 298.0 K) of guest **BP2**.

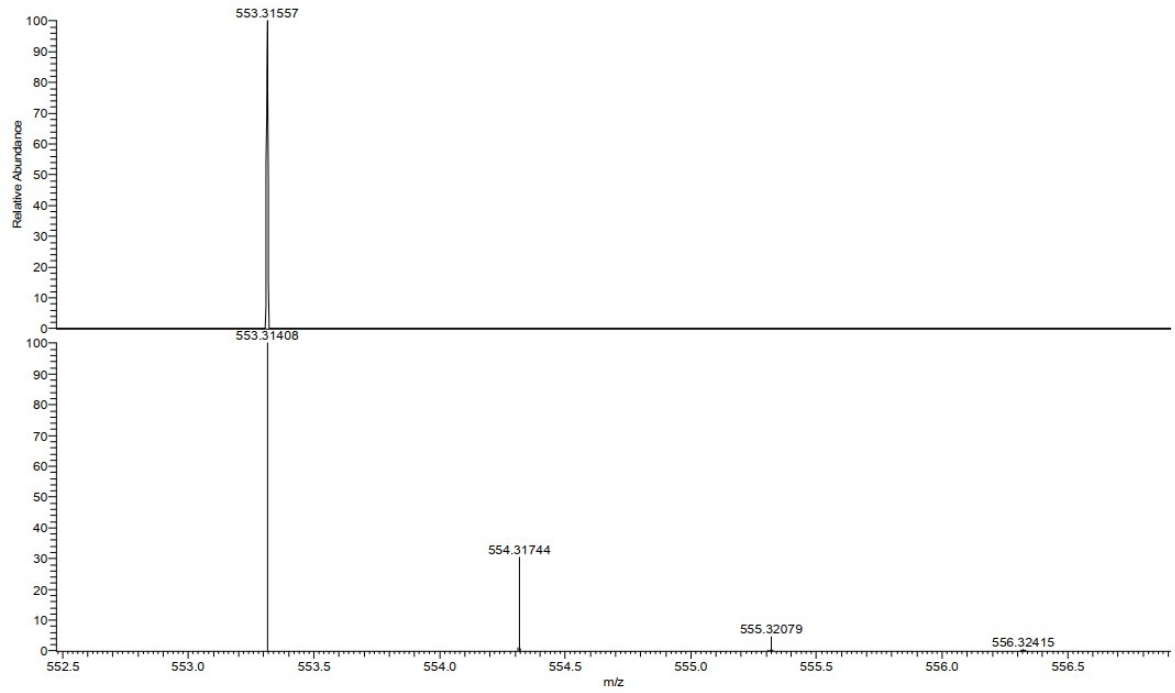

HRMS (ESI)-mass spectrum of guest **BP2**.

References

S1 Frisch, M. J.; Trucks, G. W.; Schlegel, H. B.; Scuseria, G. E.; Robb, M. A.; Cheeseman, J. R.; Scalmani, G.; Barone, V.; Petersson, G. A.; Nakatsuji, H.; Li, X.; Caricato, M.; Marenich, A. V.; Bloino, J.; Janesko, B. G.; Gomperts, R.; Mennucci, B.; Hratchian, H. P.; Ortiz, J. V.; Izmaylov, A. F.; Sonnenberg, J. L.; Williams; Ding, F.; Lipparini, F.; Egidi, F.; Goings, J.; Peng, B.; Petrone, A.; Henderson, T.; Ranasinghe, D.; Zakrzewski, V. G.; Gao, J.; Rega, N.; Zheng, G.; Liang, W.; Hada, M.; Ehara, M.; Toyota, K.; Fukuda, R.; Hasegawa, J.; Ishida, M.; Nakajima, T.; Honda, Y.; Kitao, O.; Nakai, H.; Vreven, T.; Throssell, K.; Montgomery Jr., J. A.; Peralta, J. E.; Ogliaro, F.; Bearpark, M. J.; Heyd, J. J.; Brothers, E. N.; Kudin, K. N.; Staroverov, V. N.; Keith, T. A.; Kobayashi, R.; Normand, J.; Raghavachari, K.; Rendell, A. P.; Burant, J. C.; Iyengar, S. S.; Tomasi, J.; Cossi, M.; Millam, J. M.; Klene, M.; Adamo, C.; Cammi, R.; Ochterski, J. W.; Martin, R. L.; Morokuma, K.; Farkas, O.; Foresman, J. B.; Fox, D. J. Gaussian 09 Rev. A.02, Wallingford, CT, 2013.*Journal*.

S2 T. Lu and F. Chen, Multiwfn: A multifunctional wavefunction analyzer, *Journal of Computational Chemistry*, 2012, **33**, 580-592.

S3 X.-N. Xu, L. Wang, G.-T. Wang, J.-B. Lin, G.-Y. Li, X.-K. Jiang and Z.-T. Li, Hydrogen-bonding-mediated dynamic covalent synthesis of macrocycles and capsules: New receptors for aliphatic ammonium ions and the formation of pseudo[3]rotaxanes, *Chemistry - A European Journal*, 2009, **15**, 5763-5774.

S4 J. Zhu, Q. Gao, Q. Tong and G. Wu, Fluorescent probes based on benzothiazole-spiropyran derivatives for pH monitoring in vitro and in vivo, *Spectrochimica Acta Part A: Molecular and Biomolecular Spectroscopy*, 2020, **225**, 117506.

S5 N. Papaiconomou, J. Salminen, J.-M. Lee and J. M. Prausnitz, physicochemical properties of hydrophobic ionic liquids containing 1-octylpyridinium, 1-octyl-2-methylpyridinium, or 1-octyl-4-methylpyridinium cations, *Journal of Chemical & Engineering Data*, 2007, **52**, 833-840.

S6 M. Kuroboshi, T. Shiba and H. Tanaka, Viologen as catalytic organic reductant: electro-reductive dimerization of aryl bromides in a Pd/viologen double mediatory system, *Tetrahedron Letters*, 2013, **54**, 3666-3668.

S7 A. J. Leitgeb, J. A. Feliciano, H. A. Sanchez, R. A. Allen, K. R. Morrison, K. J. Sommers, R. G. Carden, W. M. Wuest and K. P. C. Minbiole, further investigations into rigidity-activity relationships in BisQAC amphiphilic antiseptics, *ChemMedChem*, 2020, **15**, 667-670.